Mechanism of Hydrogen Sulfide-Dependent Inhibition of FeFe Hydrogenase

Christina Felbek, Federica Arrigoni, David de Sancho, Aurore Jacq-Bailly, Robert B Best, Vincent Fourmond, Luca Bertini, Christophe Léger

Mechanism of hydrogen sulfide dependent inhibition of FeFe hydrogenase

Christina Felbek (a), Federica Arrigoni (b), David de Sancho (c), Aurore Jacq-Bailly (a), Robert B. Best (d), Vincent Fourmond (a), Luca Bertini (b) and Christophe Léger (a)*

(a) Laboratoire de Bioénergétique et Ingénierie des Protéines, CNRS, Aix Marseille Université, Institut de Microbiologie de la Méditerranée, Institut Microbiologie, Bioénergies et Biotechnologie, Marseille, France

(b) Department of Biotechnology and Biosciences, University of Milano-Bicocca, Milan, Italy

(c) Polimero eta Material Aurreratuak: Fisika, Kimika eta Teknologia, Kimika Fakultatea, Euskal Herriko Unibertsitatea UPV/EHU & Donostia International Physics Center (DIPC) PK 1072, 20080 Donostia-San Sebastián, Spain

(d) Laboratory of Chemical Physics, National Institute of Diabetes and Digestive and Kidney Diseases, National Institutes of Health (NIH), Bethesda, MD, USA

* leger@imm.cnrs.fr

Abstract

The so-called FeFe hydrogenases catalyze H_2 production and oxidation at a dinuclear inorganic active site. Some of them can be natively purified in an overoxidized, O_2-resistant "H_{inact}" state, recently identified by Rodríguez-Maciá *et al*. as the product of the reaction of the enzyme with sulfide (J. Am. Chem. Soc. 140, 9346 (2018)). We used a combination of direct electrochemistry experiments with the FeFe hydrogenase from *C. reinhardtii*, site-directed mutagenesis, and molecular dynamics and DFT calculations to describe the mechanism of inhibition: the diffusion of the inhibitor in the enzyme and its subsequent reaction at the active site. We conclude that hydrogen sulfide (H_2S) inhibits the enzyme non-competitively, in a first step by replacing a conserved water molecule that is involved in proton transfer to/from the active site, and then binding to the active site as a hydrosulfide ligand (HS^-). DFT calculations with the PBE0-D3 functional successfully describe the redox state of the cubane subcluster in the resulting "H_{trans}" state. In contrast with the proposal of Rodríguez-Maciá *et al.*, our experimental and theoretical results are consistent with the reactivation involving the reduction of H_{trans}, followed by the potentiometric or catalytic re-oxidation of the enzyme. This mechanism reconciles all experimental observations and we suggest that it is common to all FeFe hydrogenases. In addition, we observe that the hydrogenases from *M. elsdenii*, *C. acetobutylicum* (CaI) and *C. pasteurianum* (CpI) are also inhibited by sulfide, but with very slow kinetics. Whereas sulfide inhibition is fully reversible, we observed an irreversible inactivation by polysulfide contaminants, which should be avoided if the hydrogenase is exposed to sulfide to prepare samples that are protected from air, e.g. for transport or storage.

Key words: hydrogenase, inhibition, protein film voltammetry, kinetics, DFT, Molecular dynamics

Introduction

The enzymes that oxidize or produce H_2 belong to one of two families, FeFe or NiFe hydrogenases.[1,2] A third class of hydrogenase uses a mononuclear Fe active site to catalyze the reversible heterolytic

cleavage of H_2 and hydride transfer to an additional substrate (methenyltetrahydromethanopterin),[3] and the enzyme nitrogenase also reductively produces H_2 as a by-product of nitrogen fixation.[4]

Here we focus on FeFe hydrogenases, whose active site, called the H-cluster, consists of a $[Fe_2(CN)_2(CO)_3(adt)]^{2-}$ (adt=azadithiolate) binuclear cluster that is covalently attached to a cubane cluster ($[4Fe4S]_H$) by a cysteine residue.[1] The vibrations of the intrinsic CO and CN^- ligands can be detected by FTIR and are the fingerprints of the catalytic intermediates. The Fe ions that are close and remote from the cubane are referred to as proximal (Fe_P) and distal (Fe_D), respectively.

In the catalytic cycle, H_2 binds to the apical binding site on Fe_D, it is heterolytically split into a terminal hydride and a proton ; the latter is transferred to the nitrogen atom of the adt ligand that bridges the two Fe ions.[5,6] Reoxidation closes the catalytic cycle. A conserved proton transfer chain, consisting in particular of a proximal cysteine, a water molecule and a glutamate residue, connects the active site to the solvent.[7–13] Although not strictly conserved,[14,15] this motif is present in all hydrogenases discussed herein.

The exact sequence of proton and electron transfers that occur at the H-cluster when H_2 is oxidized or evolved has been debated (see refs. [16,17] for recent reviews). The consensus is that H_2 binds to the H-cluster in a paramagnetic state that is called "H_{ox}", where the redox state of the Fe_2 pair is Fe(II)Fe(I) and the cubane of the H-cluster is oxidized ($[4Fe4S]_H^{2+}$). A number of states more reduced than H_{ox} have been distinguished based on their FTIR signatures. The EPR silent states that are one-electron more reduced than H_{ox} are relevant in this work, in particular the "H_{red}" state (Fe(II),Fe(I),$[4Fe4S]_H^{1+}$) and its protonated form $H_{red}H^+$ (Fe(I),Fe(I),$[4Fe4S]_H^{2+}$)[18].

The 50 kDa enzyme from *Chlamydomonas reinhardtii* (HydA), used in most of the experiments reported herein, consists of a single subunit and has no other cofactor than the conserved H-cluster.[19] However, quaternary structures and cofactor contents greatly vary among FeFe hydrogenases. For example, the two identical enzymes from the sulfate reducing bacteria *Desulfovibrio vulgaris* and *Desulfovibrio desulfuricans*[20] and the hydrogenase from *Megasphaera elsdenii* house 2 accessory FeS clusters in addition to the H-cluster ; those from *Clostridium acetobutylicum* (CaI) and *Clostridium pasteurianum* (CpI)[7] have four additional accessory clusters.

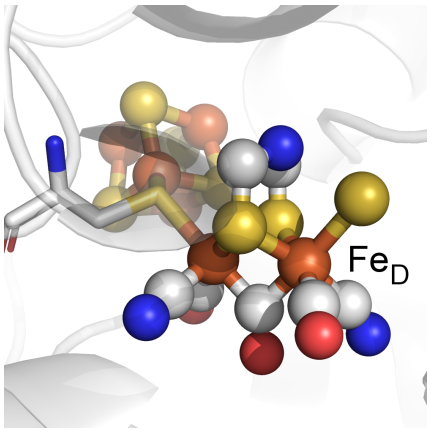

Figure 1. The structure of the H_{inact} state of the H-cluster of FeFe hydrogenase according to pdb 6SG2.[21] Note the presence of the apical sulfur ligand (yellow, top right) on the rightmost, distal Fe ion (Fe_D). This structure was obtained from a crystal of *D. desulfuricans* hydrogenase, but the structure of the H-cluster and the FTIR signature of its H_{inact} state are the same in the hydrogenases from *C. reinhardtii* and *D. desulfuricans*.[22]

Whereas most FeFe hydrogenases are O_2 sensitive,[23] those from *D. desulfuricans* and *D. vulgaris* can be purified natively in air. In that case, they are produced in a particular O_2-resistant, overoxidized, inactive state, called "H_{inact}" (or sometimes "$H_{ox,air}$"), which gives the active enzyme upon reduction.[24] Its structure and reactivity remained elusive for over 40 years, but they were disclosed very recently.[21,22] This paper focuses on the mechanism of formation and reactivation of H_{inact}.

Early investigations showed that the H_{inact} state is EPR silent. Its one electron reduction at $E_m \approx -90$ mV *vs* the standard hydrogen electrode (SHE) is fully reversible[22,25] and nearly pH-independent,[25] and gives the H_{trans} state. The results of EPR[26,27] and Mössbauer[28] investigations of *D. vulgaris* FeFe hydrogenase suggested that the cubane is oxidized in H_{inact} and reduced to the +1 state in H_{trans}.

Further reduction of H_{trans} is required to activate the enzyme to the H_{ox} state, and in reductive redox titrations of H_{inact}, an apparent E_m for the H_{trans}/H_{ox} transition was estimated around $E_m = -300$ mV *vs* SHE.[22,29] However, this reduction being irreversible (reoxidation produces neither H_{trans} nor H_{inact}), it is not possible to equate this E_m with any thermodynamic parameter. Roseboom *et al.* concluded that the H_{inact} to H_{ox} transformation most likely involves two electrons (consistent with both species being paramagnetic).[25] In contrast, based on an investigation by Mössbauer spectroscopy, Pereira *et al.* concluded that the transformation between H_{trans} and H_{ox} is not a reduction but rather involves an intramolecular electron transfer from the cubane to the binuclear cluster,[28] and indeed the current consensus is that H_{ox} (Fe(II),Fe(I),$[4Fe4S]_H^{2+}$) is isoelectronic with H_{trans} (Fe(II),Fe(II),$[4Fe4S]_H^{1+}$).

Only recently did Rodríguez-Maciá *et al.* elucidate the chemical nature of H_{inact}. They demonstrated that this state can be produced upon reaction of the active form of the enzyme with sulfide under anaerobic, oxidizing conditions.[22] In this paper, we will use the term "sulfide" to imply "H_2S + HS^-", since S^{2-} does not exist in aqueous solutions.[30]

X-ray diffraction and spectroscopy (XAS, Raman, NRVS) of the enzyme from *D. desulfuricans* in the H_{inact} state are consistent with Fe_D being bound to an additional sulfide ligand (Figure 1).[21] The sulfide occupies the H_2 binding site, which is also the initial binding site of the substrate H_2 and of the inhibitor dioxygen[23], hence the fact that H_{inact} is inactive and protected from O_2. The presence of sulfide in the growth medium of sulfate reducing bacteria offers an explanation as to why the H_{inact} state was initially observed only with the enzymes purified from these microorganisms. Rodríguez-Maciá *et al.* showed that the H_{inact} state can also be obtained *in vitro*, by exposing FeFe hydrogenase in the H_{ox} state to sulfide, followed by anaerobic oxidation. This procedure works with the recombinant enzymes from *D. desulfuricans* and *C. reinhardtii*, but not with that from *C. pasteurianum* (CpI). The latter was reported to be insensitive to Na_2S, but we mitigate this view hereafter.[21] In *Clostridium beijerinckii* FeFe hydrogenase, a similar H_{inact} state results from the coordination of a conserved cysteine to Fe_D, a process that is made possible by the particular flexibility of the loop that bears this residue.[31,32]

Regarding *D. desulfuricans* hydrogenase, the proposed inactivation mechanism of inhibition by exogenous sulfide (reproduced from ref [22] in supplementary Figure S1) begins with the binding of H_2S to the distal Fe ion in H_{ox}. The conclusion that the inhibitor is H_2S, rather than HS^-, is based on the observation that the H_{inact} state can be formed using Na_2Se only at low pH[21] (consistent with the pK_a of H_2Se being lower than that of H_2S[33]). The H_2S binding step is thermoneutral according to QM/MM calculations with a model that included the dinuclear subcluster and ten nearby residues.[21] In a subsequent, exergonic step (-4.9 kcal/mol)[21], the H_2S ligand is split into a terminal HS^- and a proton that is transferred to the amine group of the adt ligand. Deprotonation of the amine gives H_{trans}, whose one-electron oxidation gives H_{inact}, which is therefore characterized by a HS^- ligand on Fe_D (Figure 1), an oxidized cubane (consistent with the state being EPR silent), a diferrous binuclear cluster and a deprotonated amine group

Reactivation can be detected by following the FTIR signature of the sample, and also as a recovery of activity in voltammetry experiments with the enzyme directly connected to the electrode.[22] In these direct electrochemistry experiments, the reactivation appears to be fast and triggered by a reduction. It is assumed to proceed along the same pathway as inactivation: reduction of H_{inact} gives H_{trans}, which is followed by protonation and endergonic release of H_2S to give H_{ox}.[22] The hypothesis

that H_{trans} is spontaneously protonated is not consistent with the observed *weak* dependence on pH of the reduction potential of the H_{inact}/H_{trans} couple (in the pH range from 6 to 9 [25]).

The above mentioned observation that in redox titrations , H_{ox} is formed upon reduction of H_{trans}, used to be considered puzzling.[29] According to Rodríguez-Maciá *et al.*, the electron required to reduce and activate H_{trans} in the enzyme from *D. desulfuricans* is taken up by a remote accessory cluster which, through redox anti-cooperativity, forces electron transfer from $[4Fe4S]_H$ to the Fe_2 pair and H_2S release.[22] This mechanism cannot be operational in *C. reinhardtii* hydrogenase, which does not embed accessory clusters, and yet the enzymes from *D. desulfuricans* and *C. reinhardtii* can be obtained in the same H_{inact} state and behave very similarly in electrochemical studies of their reaction with sulfide.[22] This raises the question as to whether or not the reactivation of H_{inact} proceeds according to the same mechanism in all FeFe hydrogenases.

Here we describe a detailed kinetic study of the (in)activation of the enzyme from *C. reinhardtii*. We propose a mechanism, supported by DFT and MD calculations, which is consistent with all experimental evidence, including data acquired by others in previous studies of the H_{inact} state of the *D. desulfuricans* enzyme. We propose that this simple mechanism is general. Furthermore, we compare the kinetics of inhibition of *C. reinhardtii*, *M. elsdenii, C. pasteurianum* (CpI) and *C. acetobutylicum* (CaI) hydrogenases (the latter is very similar to *C. pasteurianum*), and discuss the detrimental effect of polysulfide contaminants.

Results

Electrochemistry

Potential dependence of the (in)activation

In protein film electrochemistry (PFE) experiments,[34–36] the enzyme is adsorbed onto an electrode, which is rotated into a solution of buffered pH and controlled temperature, in an electrochemical cell that is open in a glove box filled with N_2. The cell solution is flushed with H_2. Depending on the electrode potential (E), H_2 oxidation or production by the enzyme is detected as a positive or negative current, respectively, whose magnitude is proportional to turnover frequency. In the experiments described here, the inhibitor was added to the buffered solution from stock solutions of hydrosulfide (HS^-) made by dissolving Na_2S in water.[30] Chloride, which also causes high potential inactivation of FeFe hydrogenases, was omitted from all buffers used in this study (see SI for details).[37]

The equilibrium between hydrosulfide and hydrogen sulfide ($pK_a = 7.0$)[38] impacts the design of our experiments. Hydrogen sulfide is a gas under normal conditions of pressure and at room temperature. As a consequence, we expect that adding HS^- to the electrochemical cell should lead to an instant increase in the concentration of HS^- and H_2S, followed by a slow and simultaneous exponential decay of the concentration of both species as H_2S escapes from the cell solution, which equilibrates with the atmosphere of the glove box. A similar decay is observed in other experiments where a solution of either O_2, CO or CO_2 is added to the cell.[39,40] The lower the pH, the more the H_2S/HS^- equilibrium is displaced in favor of H_2S, and the faster the decay.

Figure 2A shows a series of cyclic voltammograms recorded at pH 7 with *C. reinhardtii* HydA1 FeFe hydrogenase (referred to as "*C. reinhardtii* FeFe hydrogenase" hereafter). The black signal was recorded in the absence of sulfide; the H_2-oxidation current increases as the potential is swept upward, and there is no indication of inactivation.[37] The signal in red was recorded just after the injection of 1 mM HS^-. The current decay observed as the potential becomes larger than about −100 mV reveals the sulfide-dependent inactivation of the enzyme. The current is recovered as the potential is swept down, showing that a reduction triggers reactivation. In the subsequent sweeps

(grey lines), the magnitude of the decrease in current is lower, and on the 8th scan (recorded approximately 5 min after the first scan), the high potential inactivation is no longer detected. That this change from cycle to cycle is related to H_2S escaping from the cell solution is clear from the result of the same experiment performed at higher pH (Figure 2B), where the magnitude of the high potential reversible inactivation is independent of the scan number.

Irrespective of pH, a large hysteresis is seen in the high potential range of the voltammogram after sulfide addition, showing that (in)activation is slow on the time scale of the voltammetry. We shall discuss the shapes of these voltammograms in detail below. That the magnitude of the high potential inactivation is more pronounced at a lower pH results from inactivation being faster at low pH.

Supplementary Figure S3 shows a control cyclic voltammogram (CV) recorded in the absence of enzyme. A deviation from the flat base line is seen at high potential, which reveals the direct oxidation of a sulfide-related species on the electrode. This current adds to the catalytic current and contributes to the response shown in Figure 2, resulting in the small increase in positive current observed e.g. at the moment of injection on the 1st scan at pH 9 in Figure 2B.

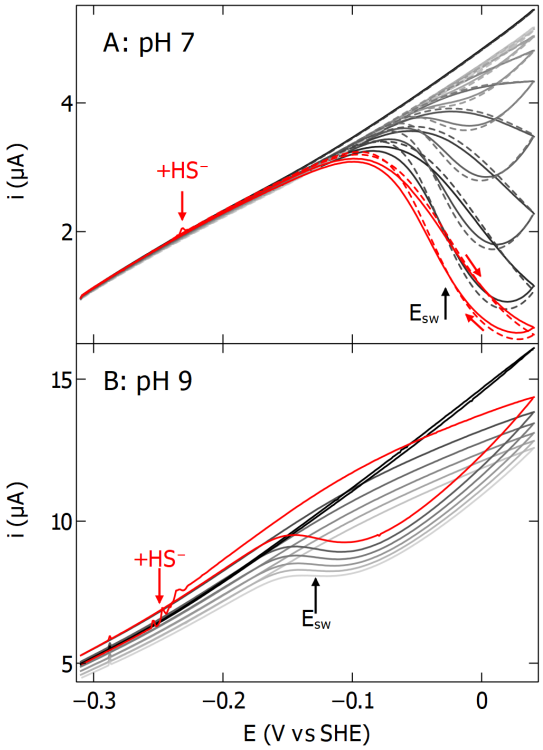

Figure 2. Series of cyclic voltammograms recorded with *C. reinhardtii* FeFe hydrogenase adsorbed onto a rotating disc pyrolytic graphite edge electrode in phosphate buffer at pH 7 (panel A) or in a mixed buffer at pH 9 (panel B) with two different enzyme films; The first CV is shown in black. The red arrows indicate the moment when 1 mM HS^- (final concentration) was added to the electrochemical cell solution on the 2nd scan (red CV). The shape of the voltammograms evolves from cycle to cycle (grey CVs) as a result of the exponential decay over time of the concentration of H_2S in the electrochemical cell. Note that the electroactive coverage is not the same in the two experiments, so the magnitudes of the signal cannot be compared. The overall current decay in subsequent scans at pH 9 results from the slow desorption of the film. The dashed line in panel A shows a fit of the same two-state kinetic model as that used to analyse the chronoamperometric data such as those in Figure 3 (see SI for fitting procedures). Scan rate = 20 mV/s, T = 5 °C, electrode rotation rate = 3000 rpm, 1 bar H_2.

The kinetics of redox-dependent (in)activation is more easily investigated in chronoamperometry (CA) experiments than in cyclic voltammetry.[41] Figure 3A shows a typical CA experiment in the presence of HS^-/H_2S, in which the H_2 oxidation current was monitored over time during a sequence of potential steps. After each potential step up or down, the current *instantaneously* changes as a result of the dependence on potential of the steady-state turnover frequency of the enzyme, and then slowly changes as a result of inactivation or reactivation ; that H_2S slowly leaves the cell results in the the observed very slow reactivations at E = 10mV. In this experiment HS^- was added at t = −27 s (relative to the first potential jump from E = −260 mV to E = +10 mV). That the rate of inactivation at a given potential depends on sulfide concentration ([HS^-] or [H_2S]) is clear from the observation that

the exponential decay in current is faster at t = 25s than at t = 125s (the electrode potential is the same, +40 mV, but the concentration of sulfide has decayed). That the concentration of inhibitor changes over time in these experiments (as a consequence of H_2S being escaping from the cell solution) allows us to probe the inactivation kinetics as a function of the inhibitor concentration in a single experiment. We have previously exploited this advantage in various studies of the reaction of FeFe hydrogenases with their gaseous substrate (H_2) and inhibitors (CO and O_2).[23,42–44]

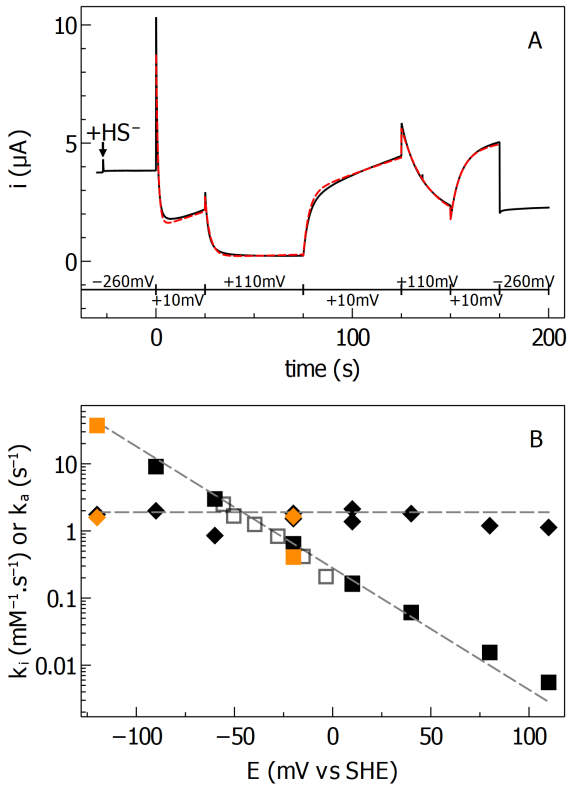

Figure 3. Panel A: Chronoamperometric (CA) experiment recorded with *Cr* FeFe hydrogenase on PG with a series of potential steps between three different values (as indicated vs SHE in the lower part of the panel). An aqueous solution of HS^- (1 mM) was injected at low potential (black arrow) 27 s before the inactivation is triggered by stepping to high oxidative potential. A simple two-state model was fitted to the chronoamperometric experiment (red dashed line).
Panel B: Inactivation and reactivation rate constants k_i (black diamonds) and k_a (black squares) at different potentials determined by fitting the model to 5 different CA experiments (like in panel A; see SI Figure S4 for the additional CA experiments and fits). The slope of the linear relation between $\log_{10}(k_a)$ and E in panel B is -F/2.3×RT, consistent with this line being the foot of a one-electron sigmoid. The rate constants obtained from fitting the CA experiments performed under 10% H_2 are shown in orange Those obtained from the CVs recorded at different scan rates are shown as open black squares (see text and SI Figure S5) The experimental conditions are the same for the data shown in the two panels: pH 7, 5°C, 3000 rpm, 1 bar H_2.

We found that a very simple two-state kinetic model can be fitted to this CA trace (and all others, recorded under similar conditions, as exemplified in SI Figure S4). The model assumes that the active enzyme inactivates with a pseudo-1st order rate constant that is proportional to the concentration of sulfide in solution. The reactivation is simply 1st order (with respect to the inactive fraction of enzymes). The fitting takes into account the fact that the inactivation rate constant k_i decreases exponentially against time as consequence of H_2S departure (as discussed in relation to Figure 2), and forces the rate constants fitted from different steps at the same potential to have the same values. See SI section 4 for details. However, the model makes no assumption regarding the mechanism of inactivation (competitive, uncompetitive or non-competitive) or the nature of the (in)activation steps (redox or non-redox): the dependence of the values of the rate constants on pH, electrode potential and [H_2] concentration will be interpreted *a posteriori*. We have used and discussed this strategy before.[41]

The dashed line in Figure 3A shows the best fit of the model to the CA trace. Repeating experiments

such as that in Figure 3A/B (SI Figure S4), varying the potential steps and fitting the model, allowed us to determine the bimolecular rate constant of inactivation k_i and the 1st-order rate constant of reactivation k_a at every potential (Figure 3B).[41] Figure 3B shows that the bimolecular rate constant k_i is independent of E, whereas k_a increases ten-fold for each 60mV decrease in E, showing that the reduction is triggered by a n = 1 electron reduction. The linear change in log(k_a) against E is the foot of a sigmoidal variation; the reduction potential E^0 of that transition cannot be measured from our data since the transition towards the plateau of the sigmoid is not seen at low potential. The typical range of rate constants that can be measured is 0.01 s^{-1} to 10 s^{-1}, and k_a is too large to be measured at E lower than −120 mV. Therefore, only an upper value of $E^0 < -120$ mV can be estimated. However, again, this value should not be compared to those obtained from reductive titrations that are not reversible.

The shape of the CVs recorded with *C. reinhardtii* hydrogenase in the presence of sulfide (Figure 2) is very dependent on scan rate (SI Fig. S5), as observed before with NiFe hydrogenases, which also reversibly inactivate under oxidative anaerobic conditions (in the absence of sulfide).[45–48] Like in the case of NiFe hydrogenase, one can relate the shape of the voltammograms and the values and dependence on E of the rate constants on (in)activation.[45–48] The shape of the CV on the sweep towards low potential is entirely defined by the dependence on potential of the rate constant of reactivation,[46–48] and independent of the exact concentration of sulfide (see e.g. Fig. 2A). The reactivation during the sweep to low potential is abrupt because the rate constant of reactivation increases exponentially as the potential decreases (*cf* Figure 3B). The "fastest" reactivation (the inflexion point in the voltammetry where di/dE is maximal) occurs at the potential (called E_{sw}, marked by a vertical black arrow in Figure 2B) where the rate at which k_a increases becomes faster than k_a itself (cf the discussion of eq. 8 in ref. [47]). This implies that k_a at $E = E_{sw}$ equals nFv, where v is the scan rate and n = 1 here. We show as open squares in Figure 3B the 6 k_a values obtained from the CVs in SI Figure S5 recorded at different scan rates; the data points match the values of k_a measured from the CA experiments, demonstrating that the value of E_{sw} is not the reduction potential E^0 of the species that reactivates, it is determined by the kinetics of reactivation.

We used the values of the (in)activation rate constants and how they depend on E to simulate the CVs in Figure 2 (dashed lines in Figure 2A), using numerical procedures that we have described before[49,50] (see details in SI section 4). The agreement between the data and the model is very good, showing that the kinetic model is relevant (in particular it captures the meaning of E_{sw}) and that the (in)activation rate constants are well determined and robust.

pH dependence of the (in)activation rate constants

We repeated the experiment in Figure 3 in the pH range 5 to 9. The results of their analyses (the fitted values of k_i and k_a) are shown in SI Figure S6.

Figure 4A shows the change in k_i, in units of s^{-1} per total concentration of sulfide (HS^-+H_2S), against pH. This rate constant decreases above pH ≈ 7, with a slope of 1 factor of ten per pH unit, which suggests that inhibitor binding is dependent upon a single protonation event, which may be the protonation of the free enzyme or of the free inhibitor. In either case the inhibition rate constant is proportional to the fraction of enzyme or inhibitor in the protonated state. Noting K_a the acidity constant of the acidic form, the change in inhibition rate constant against pH reads:

$$k_i = k_i^{\max}/(1 + 10^{-pK_a}/10^{-pH}) \quad (1)$$

That the fit of the above equation to the data (line in Figure 4A) returns pK_a = 6.8, very close to the pK_a of H_2S in water (7.0, ref. [38]), strongly suggests that the observed pH dependence reflects the protonation of HS^- in solution, and that the inhibitor is H_2S, rather than HS^-. Note that the pKa of H_2S may be different in solution and in the protein, but it is actually the H_2S/HS^- equilibrium *in solution*

that determines the effective concentration of H_2S, and the pH-dependent bimolecular inhibition rate constant. The fit also returns the low-pH limit of k_i, k_i^{max}= 3.6 s^{-1} per mM of H_2S.

Based on a previous report that H_2Se allows the formation of H_{inact} at pH 4,[21] we aimed at studying the kinetics of inactivation of *C. reinhardtii* FeFe hydrogenase using solutions made from Na_2Se. However, we could detect no inactivation in CV experiments like those shown in Figure 2 (including at pH = 4, 5 and 7, in the presence of 2 mM selenide). We also performed CA experiments at pH 5, under conditions where the enzyme film is reasonably stable (more than at pH 4), and the H_2Se/HSe^- ratio is still relatively high (about 10 %, pK_a = 3.9, ref. [33]). Upon addition of selenide to the electrochemical cell (2 or 6 mM), the current increased probably due to selenide oxidation (likewise the observed sulfide oxidation) but again no inactivation was seen (data not shown).

Figure 3B and SI Figure S6 show that the change in k_a against E is sigmoidal at all pH values, but only the foot of the sigmoid is observed, not the low potential plateau. Figure 4B shows that the 1st-order rate of reactivation is proportional to $[H^+]$. This indicates that the reactivation is dependent upon a single protonation event: either the reduction that triggers the activation is strongly coupled to a fast protonation step, or the reactivation that is coupled to the reduction step includes a rate-determining protonation step. The small deviation from the line at low pH should not be interpreted because the pH 5 data point is less reliable than the others (the film is less stable at low pH, and the values of k_a are larger, and thus more difficult to measure).

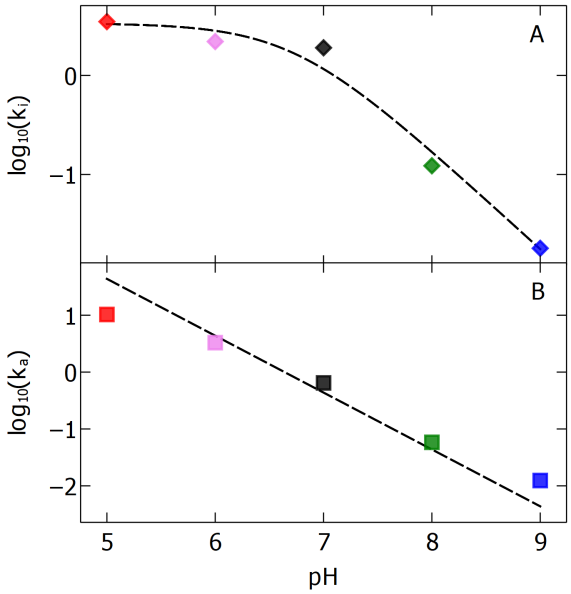

Figure 4: Dependence on pH of the rate constants of inactivation (k_i) and reactivation (k_a) (note the log scales). The data points are plotted using the same color code as in SI Figure S6 (from red at pH 5 to blue at pH 9). Panel A: pH dependence of k_i, in units of s^{-1} per total concentration of sulfide (HS^-+H_2S), and the fit of eq. (1), from which we conclude that H_2S, not HS^-, inhibits the enzyme. Panel B: pH dependence of k_a (at E = −20 mV), the line of slope -1 that is fitted to the data shows that the rate of reactivation is nearly proportional to proton concentration. Experimental conditions: 5°C, 3000 rpm, 1 bar H_2.

Non-competitive character of the initial step of in the inhibition reaction

We remind the reader that a *competitive* inhibitor resembles the substrate, and competes with it to bind to the active site. CO is a competitive inhibitor of FeFe hydrogenases.[51] An *uncompetitive* inhibitor binds to the enzyme substrate complex or to another catalytic intermediate, so that the larger the concentration of substrate, the stronger the inhibition (as observed e.g. for the inhibition of FeFe hydrogenases by chloride[37]). In contrast a *non-competitive* inhibitor decreases the activity upon binding to a site that is remote from the active site, irrespective of substrate concentration and of the catalytic state of the active site.[52] In the latter case, the concentration of substrate has no effect on the inhibition rate, and the presence of the inhibitor does not affect substrate binding (as measured by the value of the Michaelis constant). In this section, we demonstrate that the inhibition of FeFe hydrogenase by sulfide is non-competitive by showing that the inhibition rate constant is independent of the concentration of H_2, and that the Michaelis constant for H_2 is independent of the

concentration of inhibitor. The identity of the remote site where sulfide binds will be disclosed in the next section, where we show the results of the molecular dynamics simulations.

By repeating some of the experiment shown in Figure 3 and Figure S4 at pH 7 under a mixture of 10% H_2 and 90% Ar (instead of 100% H_2, SI Figure S7), we found that both k_i and k_a are independent of [H_2] (orange symbols in Figure 3B). The same is true at pH 9 (orange symbols in SI Figure S6). This result reveals that the inhibition mechanism is non-competitive. Indeed, if the inhibition were competitive, with a K_m for H_2 at 5°C around 0.25 atm. (see the results of Km measurements in Figure 5),[43] k_i would be about 3.5 times larger under 10% H_2 than under 100% H_2 (see e.g. ref [53]). If the inhibition were uncompetitive (as is the case for chloride[37]), k_i would be about 2.8 times smaller.

To confirm this finding, we measured the Michaelis constant for H_2 at E = −20 mV, pH 9 and at two different concentrations of (total) sulfide: 0 and 1 mM (the value of K_i=k_a/k_i at E = −20 mV, pH 9, equals 0.7 mM, according to the experiments in SI Figure S6). Using alkaline (instead of neutral) conditions made the concentration of sulfide nearly constant over the duration of the experiment. For this investigation, we needed to make sure that the enzyme remained equilibrated with the inhibitor: we could not use a method where the activity is measured while [H_2] is changing[43] because the (in)activation is slow ((k_i x 1 mM + k_a)$^{-1}$ ≈ 33 s) and would not keep up with the changing concentration of H_2 on the time scale of such an experiment. So we simply measured the steady-state current as a function of the concentration of H_2, as shown in SI Figure S8, and we fitted the Michaelis-Menten equation to measure the Michaelis constant. Figure 5 shows that K_m is independent of the presence of 1 mM sulfide, confirming the non-competitive character of the inhibition mechanism. Indeed, with ([H_2S]+[HS^-])/K_i ≈ 1.4, a 2.4-fold increase or decrease in K_m, compared to the value measured in the absence of inhibitor, would be observed if the inhibition were competitive or uncompetitive, respectively.

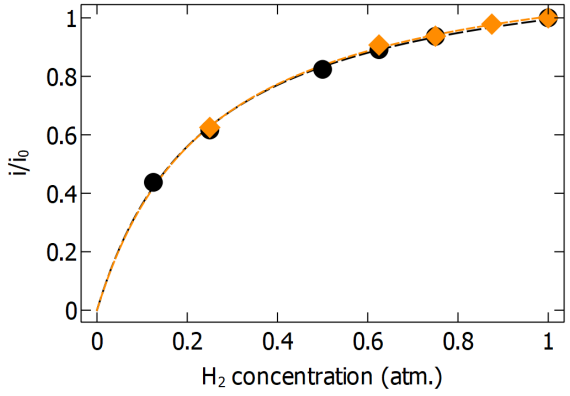

Figure 5: The presence of sulfide has no effect on the Michaelis constant relative to H_2. Steady-state current measured at different [H_2] normalized by current at [H_2]=1 atm (i_0), measured either in absence (black circle) or in the presence of 1 mM (orange diamond) sulfide. The Michaelis-Menten equation was fitted to each data set (dashed lines). The K_m values are very similar: K_m (0 mM sulfide) = 0.24 atm.; K_m(1 mM sulfide) = 0.25 atm. Experimental conditions: E = −20 mV, pH 9, 2000 rpm, 5°C (under these conditions K_i= 0.69 mM).

Comparison with other WT hydrogenases

We examined the inhibition by sulfide of the FeFe hydrogenases from *Megasphaera elsdenii*,[54] *Clostridium acetobutylicum* (CaI)[23] and *Clostridium pasteurianum* (CpI)[55]. Supplementary Figure S9A shows that in all cases, the inhibition monitored at a constant potential after injection of HS^- is followed by a reactivation as H_2S escapes from the cell solution. *C. reinhardtii* FeFe hydrogenase appears to be much more sensitive to sulfide inhibition than the three other enzymes. Fitting the kinetic model to the data in Figure S9B gave the rate constants of inhibition and reactivation reported in Table 1. The low sensitivity of *C. pasteurianum*, *C. acetobutylicum* and *M. elsdenii* FeFe hydrogenases comes from the rate constant k_i being two orders of magnitude smaller than that of *C. reinhardtii* FeFe hydrogenase. Because of this slow binding kinetics, we could not perform a detailed investigation of the potential dependence of the (in)activation rate constants.

	k_i ($mM^{-1}·s^{-1}$)	k_a (s^{-1}) at −20 mV *vs* SHE
Cr [(a)] + sulfide	1.9	0.65
Ca + sulfide	0.03	0.45
Me + sulfide	0.035	0.26
CpI + sulfide	0.045	0.25
Cr + CO	13	0.0012

Table 1. Comparison of the kinetics of inhibition by sulfide or CO of various hydrogenases, and one site-directed mutant of *Cr* FeFe hydrogenase, all at pH 7, 5°C. The value of k_i is in units of s^{-1} per mM of total sulfide (HS^-+H_2S) or CO. (a) the *Cr* WT values are consistent with the data in SI Figure S9A, but they were obtained from the potential steps experiments in Figure 3 (this value of k_i is too large to be measured at the high concentration of sulfide used for the other enzymes in SI Figure S9A).

Irreversible inactivation by polysulfide

Figure S10A shows the UV-vis spectrum of a HS^- solution freshly prepared from Na_2S under anaerobic conditions (black trace), and the spectrum of a solution of polysulfide[56] with its characteristic peak at around 300 nm (red trace).[57] Unsurprisingly, the HS^- solution contains trace amounts of polysulfides.

Supplementary Figure S10B shows the effect of either solution (added at t = 100 s) on the H_2-oxidation current of *C. reinardtii* FeFe hydrogenase in a CA experiment at −20 mV. If polysulfide is present as traces (as in all of the experiments described in this work, except SI Figure S10), the comparison of the initial and final values of the H_2 oxidation current (black trace in SI Figure S10B) shows that inhibition is mostly reversible. If polysulfide is concentrated, the inhibition is slow and mostly irreversible (red trace in SI Figure S10B).

Molecular dynamics

Intramolecular diffusion of H_2S

In order to probe the pathways that allow the H_2S molecules to reach the active site, we ran atomistic molecular dynamics (MD) simulations as in our previous work.[23] Since no experimental structure of the holo-form of the enzyme from *C. reinhardtii* is available, we used the structure of the *D. desulfuricans* enzyme (PDB code 1hfe[20]). Previous reports suggest that *D. desulfuricans* and *C. reinhardtii* hydrogenases behave similarly in terms of reaction with sulfide. The residues and proton transfer pathway that are mentioned in this work are all conserved in *D. desulfuricans*, *C. reinhardtii*, CpI and CaI hydrogenases. We chose not to use the structure of the *Clostridium pasteurianum* enzyme, which is very slowly inhibited by sulfide (Table 1).

We used the Amber03w protein force field,[58] which was optimized to work with the TIP4P/2005 water model.[59] As in our previous work, the FeS clusters were modelled using the parameters developed by Chang and Kim[60]. The simulations (Figure 6 and SI section 5.2) captured the positions of the water molecules observed in the crystals. In Figure 6B, the molecule involved in proton transfer (see table S2) is labelled W1.

In order to enhance the sampling of protein tunnels, simulations were performed in the presence of 43 H_2S molecules, corresponding to a 100 mM concentration, which were modelled using GAFF2 parameters calculated using the Parameterize web tool by De Fabritiis and co-workers.[61] The protein and ionic clusters remained stable for all the duration of our long equilibrium trajectory of ~1 μs (see SI Figures S12 and S13), suggesting the hydrogenase structure is not perturbed by the presence of H_2S.

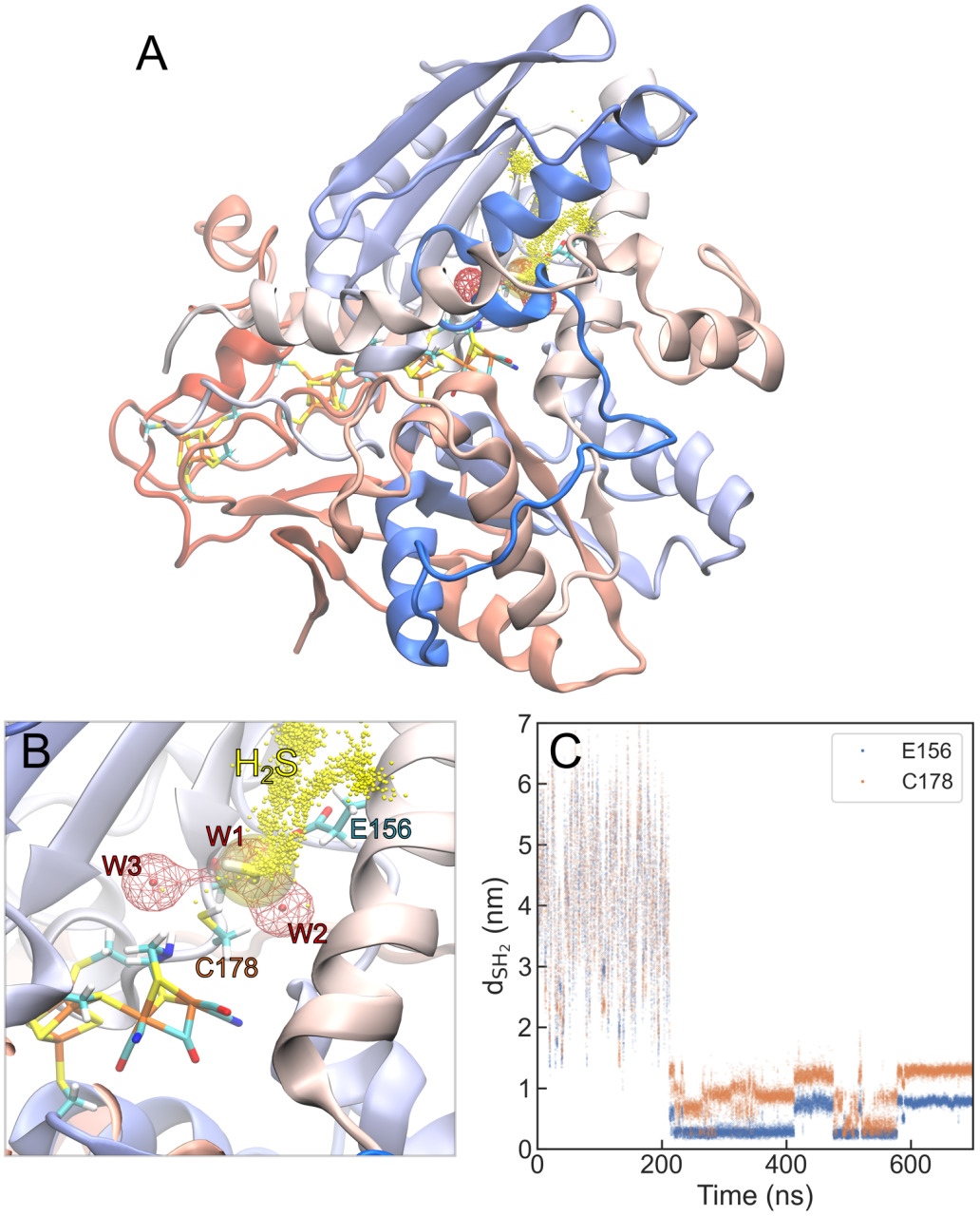

Figure 6: Diffusion of H_2S in FeFe hydrogenase. (A) Cartoon representation of *D. desulfuricans* FeFe hydrogenase, with atomic detail for metal clusters and amino acid residues of interest. We show as yellow spheres the positions of the H_2S molecules in the entry pathway through the main hydrogenase tunnel. Red spheres and surfaces correspond to the positions of three crystallographic waters in the 1HFE X-ray structure (W1: 648, W2: 20, W3: 638). (B) Detail showing a specific snapshot where the H_2S approaches the conserved water site W1, which serves as a proton relay.[7–13] Atomic detail is shown for the E156 and C178 that surround the conserved water site involved in proton transfer. (C) Time series data for the average distances between the side chains of residues E156 or C178 and the selected H_2S molecule.

The reason H_2S non-competitively inhibits the enzyme

In our simulations, we observed that the H_2S molecules bind to a number of pockets in the enzyme (see Figure 6). Specifically, after the initial 200 ns two H_2S molecules enter the main protein tunnel identified for *D. desulfuricans* hydrogenase by Nicolet et al.[20] This channel was also termed "pathway A" in MD simulations of CpI hydrogenase by Schulten et al.,[62] and was also reported by some of us to be essential for O_2 access to the H-cluster.[23] The H_2S molecules displace a thread of water molecules whose presence in the tunnel of CpI hydrogenase was noted by others before.[8] While one of the H_2S molecules occupies the protein interior only transiently, the other gas molecule keeps diffusing back and forth in the tunnel for most of the duration of the trajectory (see SI Figure S14). As shown in Figure 6B (and SI section 5), this H_2S molecule approaches the conserved water site W1, which is part of the proton transfer pathway.[7–13] These visits are captured as a decrease in the distance between the gas molecule and the two residues that flank the water site and are part of the proton transfer pathway (E156 and C178, *D. desulfuricans* hydrogenase numbering; see Figure 6C). We also note that in a 500 ns simulation trajectory performed in the absence of H_2S but with the same number of Cl^- anions, no binding event of the chloride was observed.

We hypothesize that the binding of H_2S to the water site is responsible for the above described non competitive inhibition by sulfide. Indeed, this molecule is involved in proton transfer to/from the active site, and we consider likely that the replacement of the water molecule W1 with hydrogen sulfide should disrupt this process, since the acidity constants of H_2O and H_2S in water differ by seven orders of magnitude. Moreover, this water site is remote from the H-cluster, so we expect that the binding of H_2S at that site should be independent of the redox state of the H-cluster and of the concentration of H_2; this explains the non-competitive character of the inhibition.

DFT calculations

We use DFT calculations to describe H_2S binding at the water site and the chemical events that follow: the transfer of the ligand to the H-cluster in the H_{ox} state, the proton and electron transfer steps that lead to the formation of H_{inact}, and the ligand release and reactivation that occur upon reduction.

Models and calibration

We performed most of our DFT computations on a “large” model (18 residues plus the complete H-cluster), using two distinct functionals, namely BP86-D3 and PBE0-D3, within the unrestricted broken-symmetry formalism, to properly take into account the antiferromagnetic coupling of the 4Fe4S cluster (SI section 6.1). These two functionals have been used in many previous DFT investigations of FeFe hydrogenase and other inorganic systems.[63–68] We also calculated the electronic structure and geometries of the H_{trans} and H_{inact} states using two other DFT functionals, the pure TPSS and the hybrid TPSSh (see SI section 6.5), which gave good performances in previous investigations of FeS cofactors.[69,70]

We first examined the electronic structures of H_{ox} ($Fe^{II}Fe^{I}[4Fe4S]^{2+}$), its one-electron reduced form H_{red} ($Fe^{II}Fe^{I}[4Fe4S]^{+}$) and its reduced and protonated form $H_{red}H^+$ ($2Fe^{I}[4Fe4S]^{+2}$). The computations carried out at PBE0-D3 level confirmed the redox state assignments proposed in the literature (SI section 6.2). In particular, they account for the oxidized and reduced states of the cubane subcluster in H_{red} and $H_{red}H^+$, respectively.[18] In contrast, BP86-D3 incorrectly predicts that the cubane subcluster is oxidized in H_{red} (our calculations in SI section 6.2, consistent with those described in ref. [70]). For this reason we focus in the main text on the results obtained with PBE0-D3. The comparison with BP86-D3 is discussed in SI. When required, calculations were also carried out using smaller or larger H-cluster models (SI sections 6.1 for details), and including in the model the water molecule W2 (Figure 6B and SI section 6.3.3).

Binding of H_2S to the water site

Using the large DFT model, we investigated the initial replacement of this water molecule with H_2S observed in the MD calculations; according to our hypothesis, this is the first event that inhibits the enzyme.

According to ref. [13], the aspartic acid residue E156, which flanks the water molecule in the proton transfer pathway is protonated both in the H_{ox} and $H_{red}H^+$ states. Under the assumption that E156 is protonated, our calculations show that the displacement of the H_2O molecule with H_2S is followed by proton transfer from C178 to the adt bridging ligand, resulting in the presence of HS^- at the water site (the process is endergonic by +5.5 kcal/mol, SI section 6.3.2, scheme S4).

However, since E156 is involved in proton transfer in the catalytic cycle, we expect the (de)protonation of this residue to be fast on the catalytic time scale.[8] Furthermore, (de)protonation of the residues along the chain may continue after the water site becomes occupied by the inhibitor. So there is no reason to assume a particular protonation state, and we therefore also run the calculation assuming that E156 is deprotonated. In that case, H_2S binding to the water site is followed by proton transfer from H_2S to E156, as shown in Figure 7A (overall, -5.8 kcal/mol, see SI section 6.3.1, scheme S3 for structural details). This conclusion that H_2S deprotonates at the water site if E156 is deprotonated is maintained based on calculations with the "very large" model, which included 7 additional residues around the water binding site (SI Section 6.3.1, Figure S20).

The replacement of H_2O with H_2S is exergonic even in calculations that include the water molecule W2 (SI Figures S2 and S23), irrespective of the E156 protonation state. This suggests that the second water molecule plays a minor role in the inhibition mechanism. We did not consider it further.

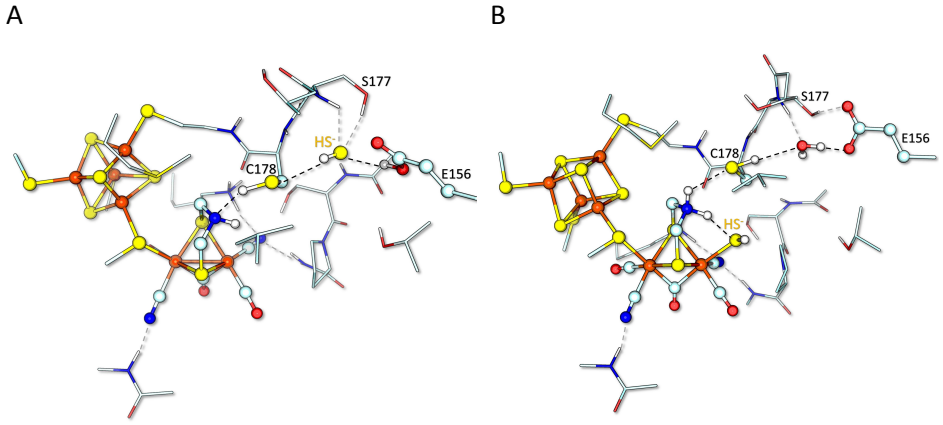

Figure 7. DFT optimized structures (PBE0-D3) of H_{ox} with HS^- bound at the water site (panel A), or after binding of H_2S to Fe_D and its splitting into HS^- and H^+ (panel B).

The binding of sulfide to Fe_D and the protonation state of H_{trans} and H_{inact}

To discuss the following DFT results, as in ref. [37], we used notations such as "H_{red}/HS^-" or "$H_{red}/HS^-/H^+$" to denote the chemical composition of the different intermediates, without prejudging their structure. "H_{overox}" and "H_{red}" are one electron more oxidized or reduced than H_{ox}, respectively. "$H_{red}/HS^-/H^+$", for example, corresponds to a state where either HS^- and H^+ or H_2S are bound, somehow, to the reduced H-cluster.

We calculated in SI Section 6.3 that irrespective of the exact number of protons (starting from either protonated or deprotonated E156), the initial binding of H_2S to the water site is followed by the very exergonic binding of HS^- to Fe_d and protonation of the adt bridge, to form a species that we call

$H_{ox}/HS^-/H^+$ (Figure 7B) with valence-delocalized state $2Fe^{1.5}$ and oxidized $[4Fe4S]^{2+}$ cluster. The energy of this process is ≈ -16 kcal/mol at PBE0-D3 level irrespective of the protonation state of E156.

The formation of $H_{ox}/HS^-/H^+$ from H_{ox} and H_2S is much more exergonic than the binding of other substrates such as H_2, H_2O or Cl^- (SI section 6.4, Table S4), as reported before by Rodríguez-Maciá *et al*. at QM/MM level and using a different protocol for the QM part (TPSSh-D3BJ functional plus ZORA relativistic approximation and def2-TZVP basis set).[21] This is confirmed also from calculations performed on our simpler, small model (SI Section 6.1), which focuses on the Fe_D region. We did not attempt to calculate the energy barriers for the binding steps.

We compared the DFT structures of two candidates for H_{trans}, which should contain a reduced cubane cluster according to previous spectroscopic investigations,[26,27] namely $H_{ox}/HS^-/H^+$ and the deprotonated species H_{ox}/HS^- (SI section 6.5). Regarding the deprotonated species H_{ox}/HS^-, calculations with the large model identified two isomers differing only by the localisation of an electron on the cubane or on the dinuclear cluster. The two isomers are observed irrespective of the functional that is used (PBE0-D3, BP86-D3, TPSS-D3 and TPSSh-D3), although their relative stability depends on the functional. With PBE0-D3, the isomer with the reduced cubane is 6.9 kcal/mol more stable than the other isomer (SI Section 6.5), even without considering factors (e.g. protonation) that could compensate for the charge accumulation on the 4Fe4S cluster.[71–73] In contrast, no stable form with a reduced cubane was observed with the protonated species $H_{ox}/HS^-/H^+$. Since the EPR spectra of H_{trans} indicate that the cubane is reduced,[26,27] and consistent with previous assumptions,[22] we consider that the deprotonated species H_{ox}/HS^- is the most likely stoichiometry of H_{trans}.

H_{inact} is one-electron more oxidized than H_{trans}.[25] In SI Section 6.5 we report the DFT electronic structure of H_{inact} (H_{overox}/HS^-, Fe(II)Fe(II) $[4Fe4S]^{2+}$), and the comparison between the calculated bond distances and those deduced from the X-ray structure shown in Figure 1.[21]

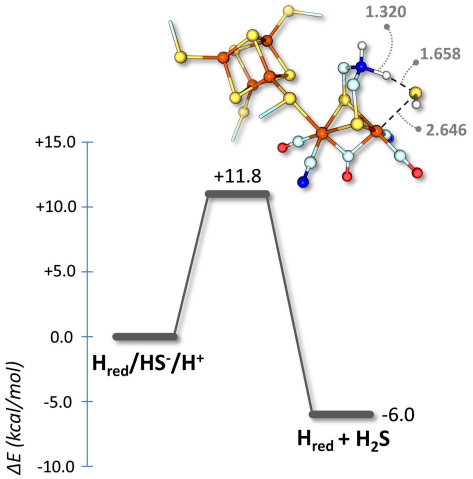

Figure 8. DFT calculation of the release of H_2S from the $H_{red}/HS^-/H^+$ form of the H-cluster. The numbers indicate the changes in total energy calculated using the PBE0-D3 functional and the large DFT model, which included 14 residues in addition to the H-cluster. Distances are indicated in Å.

Reactivation

Following early evidence that reactivation occurs upon the reduction of H_{trans}, using the above conclusion that H_{trans} is H_{ox}/HS^-, and using our finding that reactivation is coupled to protonation (Figure 4B), we conclude that the species whose formation triggers the reactivation in *C. reinhardtii* hydrogenase should be $H_{trans} + 1e^- + 1H^+$, that is $H_{red}/HS^-/H^+$. DFT calculations indicate that H_2S release from such species is exergonic (-9.5 kcal/mol, Figure 8 and SI Section 6.6) Considering only the initial dissociation of H_2S from Fe_D (and not the following transport of H_2S in the protein), we calculated an activation barrier of +11.8 kcal/mol. The mechanism of the H_2S release from $H_{red}/HS^-/H^+$ is concerted with the concomitant N-H and Fe-SH bonds elongation.

Starting with the alternative (protonated) structure of H_{trans}, $H_{ox}/HS^-/H^+$, reduction and protonation also results in the release of H_2S, but now this is a barrierless process (SI section 6.6), which we consider less consistent with the observed rate of reactivation.

That the formation of H_{red} upon reactivation was not observed in FTIR experiments is discussed below.

Discussion

There is recent evidence that the inactive and O_2-protected H_{inact} state of FeFe hydrogenase is obtained by exposing the enzyme to sulfide and oxidizing it under anaerobic conditions. Sulfide ends up as a ligand on the distal Fe of the H-cluster (Figure 1).[21,22] The enzymes from *D. desulfuricans* and from *C. reinhardtii* show the same H_{inact} FTIR signature, and behave the same in electrochemical investigations in the presence of sulfide[22], so there is no reason to think that the mechanism of (in)activation by sulfide is different. However it has been proposed that the reduction of the accessory clusters of *D. desulfuricans* is required to allow the release of H_2S from the H_{trans} state, and studying the enzyme from *C. reinhardtii*, which embeds no accessory clusters, should be particularly useful to investigate the potential role of these clusters in the reactivation process. We performed a detailed kinetic investigation of the reaction of the enzyme from *C. reinhardtii* with sulfide, which we combined with MD and DFT calculations. We propose a revised mechanism of formation and reactivation of the H_{inact} state that is consistent with all experimental evidence, including investigations of the enzyme from *D. desulfuricans*, and which does not rely on the reduction of the accessory clusters. We suggest that this mechanism may actually be general for all FeFe hydrogenases.

In short, the mechanism that we propose involves the diffusion of H_2S through the protein until it replaces a water molecule involved in proton transfer, on a site that is slightly remote from the H-cluster (hence our observation that inhibition is non-competitive); in a subsequent step the ligand is transferred to the apical coordination site on the distal Fe. As proposed before,[22] deprotonation gives the stable state H_{trans}, whose one-electron oxidation gives H_{inact}. Rodríguez-Maciá *et al.* suggested that, at least in the case of the enzyme from *D. desulfuricans*, the reactivation of H_{trans} is triggered by the reduction of an accessory cluster, which induces H_2S release from the distal Fe by an anti-cooperative, long distance interaction with the H-cluster. Of course this mechanism cannot apply in the case of the enzyme from *C. reinhardtii*, but we show that reactivation can actually occur after the H_{trans} state is one-electron reduced; the final product is still isoelectronic with H_{trans}, because of either the potentiometric re-oxidation or the auto-oxidation of the reduced states of the H-cluster in the absence of H_2 (as reported before by Stripp *et al*.[14,74,75]). We consider likely that this simple mechanism also applies in the case of *D. desulfuricans* hydrogenase.

Here we discuss the experimental and computational evidence for each of the events in this mechanism, and the thermodynamics of the (in)activation reaction.

That H_2S is the inhibitor, rather than HS^-, was previously inferred from the observation that H_{inact} can also be formed from H_2Se, but only under more acidic conditions than with H_2S. We could not detect the inhibition by H_2Se in PFE, but the pH dependence of the bimolecular rate constant of inhibition in Figure 4A is indeed quantitatively consistent with H_2S being the molecule that inhibits the enzyme. That the rate constant of inhibition by H_2S (k_i^{max}= 3.6 $s^{-1}{\cdot}mM^{-1}$ at 5 °C in the enzyme from *C. reinhardtii* FeFe hydrogenase) is of the same order of magnitude as the rate of inhibition by CO (13 $s^{-1}mM^{-1}$ under the same conditions, Table 1) and orders of magnitude faster than the rate of inhibition by chloride (around 1 $s^{-1}{\cdot}M^{-1}$ at 2°C, same enzyme[37]) suggests that the protein hinders (but does not prevent[37]) the penetration of charged ligands. We have not attempted to run simulations to examine the penetration of HS^- in the enzyme, but we observed that unlike hydrogen sulfide,

chloride anions do not penetrate the enzyme in the 500 ns time scale of our MD simulations, consistent with the energetic penalty for burying a charge in the protein being large.

If the initial step in the inhibition reaction were the binding of H_2S to the distal Fe of the H-cluster, which is also the binding site for the substrate H_2, the inhibition would be competitive. In contrast, our observation that the inhibition by sulfide is *non-competitive* (cf the discussion of Figure 3B and Figure 5) indicates that H_2S *initially* inhibits the enzyme by binding to a site that is remote from the active site H-cluster. The molecular dynamics simulations of the transport of H_2S in *D. desulfuricans* hydrogenase reported in this work (Figure 6) identifies this initial binding site: the results suggest that H_2S diffuses along "pathway A" (the proposed diffusion pathway for other small ligands such as O_2)[23,62] and then approaches a conserved water site between C178 and E156 (*D. desulfuricans* hydrogenase numbering). H_2S binding to the water site is allowed according to DFT calculations (Figure 7A). This water molecule is part of the proton transfer pathway that involves C178 and E156,[7,8,12,13] so its replacement with H_2S, whose proton transfer properties are significantly different from H_2O, should inactivate the enzyme. This binding site is 8 Å away from the substrate binding site on Fe_D, which explains the observed non-competitive character of the inhibition.

After this initial binding step, the sulfide ligand is transferred to the apical site of the distal Fe. Electrochemistry cannot detect this transformation between the two forms of the enzyme (with the sulfide ligand either bound at the water site or on the H-cluster), because both forms are inactive, but the reaction was studied by DFT. That the sulfide/water binding site is flanked by residues involved in proton transfer, which must easily (de)protonate on the time scale of turnover, makes uncertain the exact number of protons that should be considered in a detailed DFT investigation of the reactivity of H_2S. If aspartate 156 (*D. desulfuricans* hydrogenase numbering) is initially deprotonated, the DFT calculations using large models suggest that deprotonation can occur at the water site (Figure 7A, SI scheme S3) before HS^- binds Fe_D. Else, various reaction pathways can be proposed (SI Scheme S4), but the same final product, with HS^- bound to Fe_d and a protonated adt ligand ("$H_{ox}/HS^-/H^+$" in Figure 9), can be formed independently of the proton count. Consistent with previous DFT results,[21] this species is very stable, irrespective of which model and which functional are used (SI Table S4).

According to EPR[26,27] and Mössbauer[28] investigations of *D. desulfuricans* hydrogenase, the cubane subcluster is reduced in the H_{trans} state. Only with the deprotonated H_{trans} model H_{ox}/HS^- could we observe in the calculations that the [4Fe4S] subcluster is reduced, irrespective of the functional (PBE0-D3, BP86-D3, TPSS-D3 or TPSSh-D3, SI Section S6.5). According to DFT, two isomers of H_{trans} are actually stable, $Fe^{II}Fe^{I}[4Fe4S]^{2+}$ and $Fe^{II}Fe^{II}[4Fe4S]^{+}$, which only differ by the localisation of the charge. The relative stability of the two states depends on the functional. We also consider likely that it should be affected by the protein environment of the cubane sub-cluster or the presence of additional accessory clusters (as in *D. desulfuricans* hydrogenase, the only enzyme for which the redox state of the cubane in the H_{trans} state has been investigated).

Our DFT calculations with a large model and the BPE0-D3 functional could therefore reproduce for the first time the experimentally observed variations in the redox state of the cubane subcluster, not only between H_{ox} and H_{trans}, but also between H_{red} and $H_{red}H^+$: we also calculated the internal electron transfer from the cubane subcluster to the binuclear subcluster upon protonation of H_{red} that was proposed based on FTIR investigations[18] (SI Section S6.2).

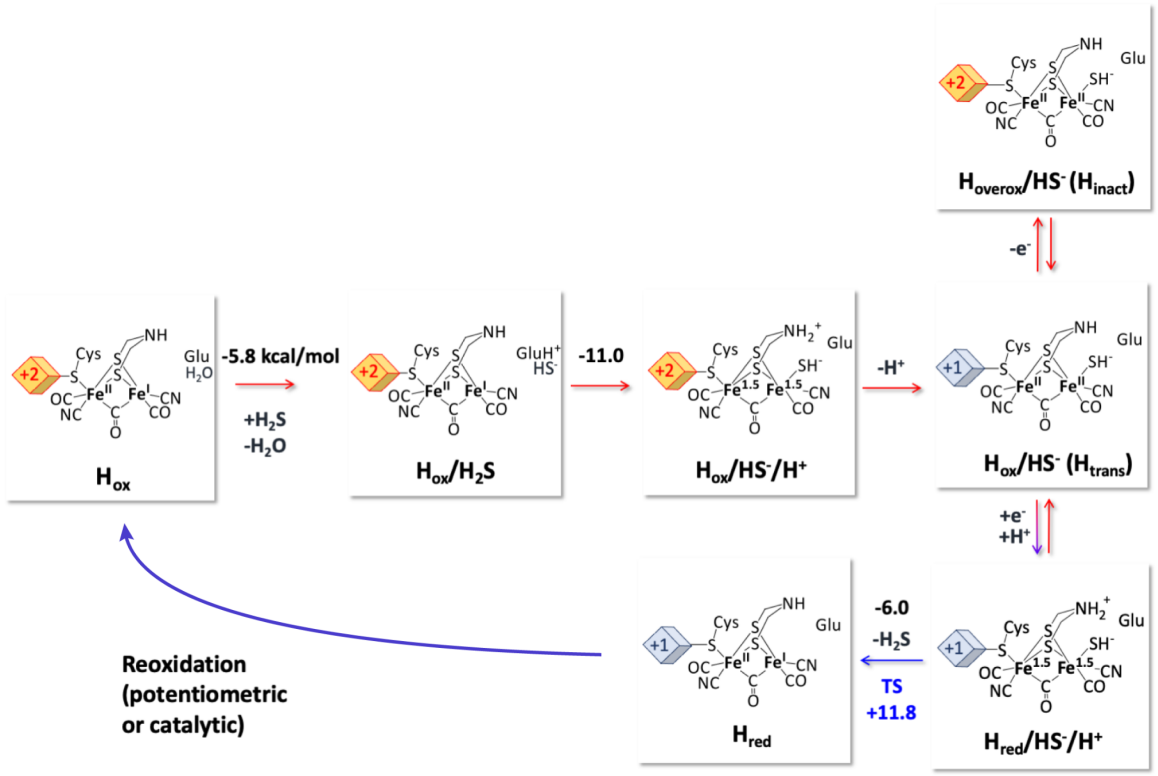

Figure 9. The proposed mechanism of inhibition of FeFe hydrogenase by H_2S, showing the binding of H_2S to the water site, then to the Fe_D site of H_{ox} as a HS^- ligand. Deprotonation gives H_{trans}, which exists in DFT calculations as two isomers; in one of them the cubane is reduced. Oxidation gives H_{inact}. We show that the reduction and protonation of H_{trans} gives a species that releases H_2S in an activated process (Figure 8), resulting in H_{red}, which can be re-oxidized by the electrode of the electrochemical cell or auto-oxidized to H_{ox} in the absence of H_2. The numbers indicate the changes in energy calculated using the PBE0-D3 functional, a large DFT model that included 14 residues in addition to the H-cluster. The numbers in blue indicate the transition state energy of the release of H_2S.

H_{inact} ("H_{overox}/HS^-" in Figure 9) is the one-electron oxidation production of H_{trans}, and reactivation involves the reverse one-electron reduction of H_{inact} to H_{trans}. This reduction is not coupled to protonation in the pH range 6 to 9.[25]

We consider it unlikely that the reactivation of H_{trans} is due to its spontaneous protonation and the release of H_2S (as in Figure S1). Indeed, H_{trans} is stable on the time scale of a redox titration (many minutes)[21,25], H_2S binds strongly to H_{ox} (according to DFT calculations in this work and in ref. [21]), and a reduction of H_{trans} is required to activate the enzyme.[22,26,27,29]

In contrast with the hypothesis in ref [22] that the electron required to activate H_{trans} is taken up by an accessory cluster (which is not present in *C. reinhardtii* hydrogenase), we propose that the reactivation follows up the reduction of the H-cluster in the H_{trans} state (Figure 9). This latter mechanism is consistent with the above conclusion that H_{trans} is kinetically stable. The electrochemical data in Figure 4B (and SI Figure S6) indicate that the one-electron reduction that triggers reactivation is coupled to protonation. Our DFT calculations show that reduction and protonation of H_{trans} is followed by the exergonic release of the inhibitor. This release is activated, consistent with experiments where the reactivation process appears to be rather slow (Figure 3B). The reactivation product should be H_{red}, or $H_{red}H^+$ depending on pH, as indeed observed in the

chemical reduction of H_{inact} described in Fig. 2 of ref [22]. From the latter observation, it cannot be decided if $H_{red}H^+$ is directly obtained from the reduction of H_{trans} (like we propose), or if H_{ox} is formed first, and then further reduced by the chemical reductant in excess. That H_2S binds more strongly to H_{ox} than to the reduction product of H_{trans} implies that H_{trans} has lower reduction potential than H_{ox}; therefore, under a given pressure of H_2S and at equilibrium, the conditions that allow the reduction of H_{trans} (and the subsequent formation of $H_{red} + H_2S$) should be too reducing to allow the reoxidation of H_{red} to H_{ox}.[76] And yet, in potentiometric reductions of H_{inact}, it has been observed that H_{ox} is obtained from the reduction of H_{trans} (e.g. Figure 2 in ref. [26], Figure 3 in ref. [25], Figure S2 in ref. [22]). The fate of the species formed upon reduction of H_{trans} should be very dependent on the experimental conditions, in particular whether sulfide is present in solution, whether the potential is controlled, and whether equilibrium is reached. In typical redox titration experiments, in which H_{trans} is reduced in the absence of sulfide (Figure 3 in ref. [25], Figure S2 in ref. [22]), the release of H_2S from the reduced state is thermodynamically very favorable, and should pull the reduction of H_{trans}; this may occur at a potential that is high enough that after H_2S is released, H_{red} is reoxidized to H_{ox} by the electrode or the mediator. In these experiments, the reoxidation of H_{ox} to H_{inact} is not possible because the stoechiometric release of H_2S results in a concentration of H_2S in solution that is too small to allow re-binding to H_{ox}. In addition to electrochemical reoxidation, catalytic turnover also interconverts H_{red} and H_{ox}; that this conversion is out of equilibrium invalidates the above argument about the thermodynamics of the binding of H_2S to the H-cluster (which suggested that H_{red} should be the product of the reductive reactivation). Catalytic interconversion between H_{red} and H_{ox} occurs in the electrochemical experiments reported here, but also in a FTIR cell: indeed, it has been observed that H_{red} and $H_{red}H^+$ are spontaneously auto-oxidized to H_{ox} by catalytic turnover in the absence of H_2.[14,74,75] Auto-oxidation of H_{red} should involve disproportionation, which is probably easy in the FTIR cell where the enzyme concentration is very large and bimolecular reactions should be fast. Whichever mechanism we consider, the spontaneous re-oxidation of H_{red} or $H_{red}H^+$ simply solves the paradox: reactivation follows up the reduction of H_{trans}, but the final product is isoelectronic with H_{trans}.

Significant differences between the sulfide sensitivity of distinct FeFe hydrogenases have been observed. Rodríguez-Maciá *et al.* reported that *Clostridium pasteurianum* (CpI) hydrogenase is not inhibited by sulfide and does not form the H_{inact} state, unlike the enzymes from *D. desulfuricans* and *C. reinhardtii*.[22] On our side, we did observe the inhibition by sulfide of the FeFe hydrogenases from *M. elsdenii* (Me),[54] *C. acetobutylicum* (CaI),[23] and *C. pasteurianum* (CpI)[55] (SI Figure S9) although with a 100-fold slower binding kinetics (Table 1) than for *C. reinhardtii*, and thus a much smaller affinity for sulfide. The enzymes from *D. desulfuricans* and *C. reinhardtii* are also more quickly inhibited by CO and O_2 than *C. acetobutylicum* and *M. elsdenii* hydrogenases (cf Table 1 in ref [49] and Table S3 in ref [77]) : these differences may simply reflect a difference in the kinetics of diffusion through the protein which still needs to be understood, but there is no reason to assume that the (in)activation mechanism should be different.

Finally, we note that exposure to sulfide followed by oxidation has been proposed as a way to protect the hydrogenase from *C. reinhardti* from oxygen, until the enzyme is reactivated by reduction under anaerobic conditions.[78] The presence of polysulfide in solutions of H_2S/HS^- is difficult to avoid,[57] but we found that fresh solutions of HS^- must be used to observe reproducible inactivation traces and full reactivation after H_2S is flushed from the electrochemical cell. We attributed the partly irreversible inactivation that we saw in preliminary experiments to a contamination by polysulfide (see the discussion of SI Figure S10). This contamination should probably be also avoided if the goal is to protect the enzyme before aerobic storage.

In conclusion, we have investigated the complex mechanism of reaction of H_2S with FeFe hydrogenase, showing that it initially inhibits the enzyme by binding non-competitively, remotely from the active site. This information comes from the characterization of the kinetics of inactivation and MD simulations of H_2S diffusion in the enzyme, and could not be reached from spectroscopic

investigations of the H-cluster. The subsequent binding of sulfide to the active site in the H_{ox} state is strongly favored, but reactivation is spontaneous after transient reduction which forms the H_{red} redox state. Like in the case of *Clostridium beijerinckii* FeFe hydrogenase, where residues that are remote from the active site strongly influence the mobility of the nearby cysteine and its binding to Fe_D,[31] we observed here that sulfide inhibition is strongly dependent on the proteic environment of the H-cluster and varies across different WT enzymes. This illustrates again the control on the reactivity of an inorganic active site that can be provided by the protein matrix.

Supplementary information

The Supporting Information is available free of charge on the ACS Publications website. Section S1 and Fig S1, The mechanism proposed by Rodríguez-Maciá et a.. Section S2: the conserved water binding site. Section S3 Purification of Cr HydA1. Section S4: Electrochemistry methods and additional data. Section S4.1 Preparation of HS^-, HSe^- and polysulfide solutions. Section S4.2 Electrochemical set-up. controlling H_2 concentration in the electrochemical cell, removal of the capacitive contribution to the current. Section S4.3 Analysis of the PFE data: analysis of the potential-steps CA data (main text Figure 3), fitting a kinetic model to the voltammograms in Figure 2, analysis of the experiments at constant potential. Section S4.4 Additional figures. Fig S3 : Direct oxidation of sulfide on the PGE. Fig S4 Additional potential steps experiments at pH 7. Fig S5: Dependence of E_{sw} on scan rate. Fig S6: pH dependence of k_i and k_a. Fig S8: Examples of CA experiments at different H_2 concentrations for the Km determination shown in Figure 5. Fig S9 Comparison of CaI, CpI, Me and Cr WT FeFe hydrogenases. Fig S10 The characterization and effect of polysulfide. Section S5: MD simulations. Section S5.1 methods, section 5.2 Solvation, section S5.3 Penetration of H_2S. Section 6: DFT additional data. Section 6.1 DFT level of theory and models. Section 6.2 Calibration of the DFT predictions. Section 6.3 H_2S at the conserved water site, and its transfer to Fed. Section 6.4 Substrate and inhibitors binding to Hox. Section 6.5 Characterization and assignment of H_2S and SH^- bound species. Section 6.6 H_2S release from reduced states (reactivation). Section 6.7 and separate file: Models xyz coordinates

Acknowledgements

We thank Thomas Happe (Bochum), Marc Fontecave (Paris), Vincent Artero (Grenoble), Isabelle Meynial (Toulouse) and their group members, for preparing the samples of *Megasphaera elsdenii*, *Clostridium acetobutilicum* (CaI), and *Clostridium pasteurianum* (CpI) hydrogenases used in the experiments in SI figure S9. We thank Marianne Guiral for her advice with the polysulfide experiments (figure S10). The work in Marseille was supported by CNRS, Aix Marseille Université and the Excellence Initiative of Aix-Marseille University – A*MIDEX, a French “Investissements d’Avenir” programme (ANR-11-IDEX-0001-02). The French authors are part of the French bioinorganic chemistry network. Financial support to DDS comes from Eusko Jaurlaritza (Basque Government) through the project IT1254-19, Grants RYC-2016-19590 and PGC2018-099321-B-I00 from the Spanish Ministry of Science and Universities through the Office of Science Research (MINECO/FEDER). RBB receives support from the Intramural Research Program of the National Institute of Diabetes and Digestive and Kidney Diseases of the National Institutes of Health. For DFT calculations, we acknowledge CINECA for the availability of high-performance computing resources as part of the agreement with the University of Milano-Bicocca.

Bibliography

(1) Lubitz, W.; Ogata, H.; Rüdiger, O.; Reijerse, E. Hydrogenases. *Chem. Rev.* **2014**, *114* (8), 4081–4148. doi: 10.1021/cr4005814

(2) Fontecilla-Camps, J. C.; Volbeda, A.; Cavazza, C.; Nicolet, Y. Structure/function Relationships of [NiFe]- and [FeFe]-Hydrogenases. *Chem. Rev.* **2007**, *107* (10), 4273–4303. doi: 10.1021/cr050195z

(3) Shima, S.; Pilak, O.; Vogt, S.; Schick, M.; Stagni, M. S.; Meyer-Klaucke, W.; Warkentin, E.; Thauer, R. K.; Ermler, U. The Crystal Structure of [Fe]-Hydrogenase Reveals the Geometry of the Active Site. *Science* **2008**, *321* (5888), 572–575. doi:

10.1126/science.1158978
(4) Hoffman, B. M.; Lukoyanov, D.; Yang, Z.-Y.; Dean, D. R.; Seefeldt, L. C. Mechanism of Nitrogen Fixation by Nitrogenase: The next Stage. *Chem. Rev.* **2014**, *114* (8), 4041–4062. doi: 10.1021/cr400641x
(5) Berggren, G.; Adamska, A.; Lambertz, C.; Simmons, T. R.; Esselborn, J.; Atta, M.; Gambarelli, S.; Mouesca, J. M.; Reijerse, E.; Lubitz, W.; Happe, T.; Artero, V.; Fontecave, M. Biomimetic Assembly and Activation of [FeFe]-Hydrogenases. *Nature* **2013**, *499* (7456), 66–69. doi: 10.1038/nature12239
(6) Silakov, A.; Wenk, B.; Reijerse, E.; Lubitz, W. (14)N HYSCORE Investigation of the H-Cluster of [FeFe] Hydrogenase: Evidence for a Nitrogen in the Dithiol Bridge. *Phys. Chem. Chem. Phys.* **2009**, *11* (31), 6592–6599. doi: 10.1039/b905841a
(7) Peters, J. W.; Lanzilotta, W. N.; Lemon, B. J.; Seefeldt, L. C. X-Ray Crystal Structure of the Fe-Only Hydrogenase (CpI) from Clostridium Pasteurianum to 1.8 Angstrom Resolution. *Science* **1998**, *282* (5395), 1853–1858. doi: 10.1126/science.282.5395.1853
(8) Long, H.; King, P. W.; Chang, C. H. Proton Transport in Clostridium Pasteurianum [FeFe] Hydrogenase I: A Computational Study. *J. Phys. Chem. B* **2014**, *118* (4), 890–900. doi: 10.1021/jp408621r
(9) Cornish, A. J.; Gärtner, K.; Yang, H.; Peters, J. W.; Hegg, E. L. Mechanism of Proton Transfer in [FeFe]-Hydrogenase from Clostridium Pasteurianum. *J. Biol. Chem.* **2011**, *286* (44), 38341–38347. doi: 10.1074/jbc.M111.254664
(10) Hong, G.; Cornish, A. J.; Hegg, E. L.; Pachter, R. On Understanding Proton Transfer to the Biocatalytic [Fe-Fe](H) Sub-Cluster in [Fe-Fe]H(2)ases: QM/MM MD Simulations. *Biochim. Biophys. Acta* **2011**, *1807* (5), 510–517. doi: 10.1016/j.bbabio.2011.01.011
(11) Ginovska-Pangovska, B.; Ho, M.-H.; Linehan, J. C.; Cheng, Y.; Dupuis, M.; Raugei, S.; Shaw, W. J. Molecular Dynamics Study of the Proposed Proton Transport Pathways in [FeFe]-Hydrogenase. *Biochim. Biophys. Acta* **2014**, *1837* (1), 131–138. doi: 10.1016/j.bbabio.2013.08.004
(12) Duan, J.; Senger, M.; Esselborn, J.; Engelbrecht, V.; Wittkamp, F.; Apfel, U.-P.; Hofmann, E.; Stripp, S. T.; Happe, T.; Winkler, M. Crystallographic and Spectroscopic Assignment of the Proton Transfer Pathway in [FeFe]-Hydrogenases. *Nat. Commun.* **2018**, *9* (1), 4726. doi: 10.1038/s41467-018-07140-x
(13) Senger, M.; Eichmann, V.; Laun, K.; Duan, J.; Wittkamp, F.; Knör, G.; Apfel, U.-P.; Happe, T.; Winkler, M.; Heberle, J.; Stripp, S. T. How [FeFe]-Hydrogenase Facilitates Bidirectional Proton Transfer. *J. Am. Chem. Soc.* **2019**, *141* (43), 17394–17403. doi: 10.1021/jacs.9b09225
(14) Land, H.; Sekretareva, A.; Huang, P.; Redman, H. J.; Németh, B.; Polidori, N.; Mészáros, L. S.; Senger, M.; Stripp, S. T.; Berggren, G. Characterization of a Putative Sensory [FeFe]-Hydrogenase Provides New Insight into the Role of the Active Site Architecture. *Chem. Sci.* **2020**. doi: 10.1039/D0SC03319G
(15) Chongdar, N.; Birrell, J. A.; Pawlak, K.; Sommer, C.; Reijerse, E. J.; Rüdiger, O.; Lubitz, W.; Ogata, H. Unique Spectroscopic Properties of the H-Cluster in a Putative Sensory [FeFe] Hydrogenase. *J. Am. Chem. Soc.* **2018**, *140* (3), 1057–1068. doi: 10.1021/jacs.7b11287
(16) Kleinhaus, J. T.; Wittkamp, F.; Yadav, S.; Siegmund, D.; Apfel, U.-P. [FeFe]-Hydrogenases: Maturation and Reactivity of Enzymatic Systems and Overview of Biomimetic Models. *Chem. Soc. Rev.* **2020**. doi: 10.1039/d0cs01089h
(17) Birrell, J. A.; Rodríguez-Maciá, P.; Reijerse, E. J.; Martini, M. A.; Lubitz, W. The Catalytic Cycle of [FeFe] Hydrogenase: A Tale of Two Sites. *Coord. Chem. Rev.* **2021**, *449*, 214191. doi: 10.1016/j.ccr.2021.214191
(18) Sommer, C.; Adamska-Venkatesh, A.; Pawlak, K.; Birrell, J. A.; Rüdiger, O.; Reijerse, E. J.; Lubitz, W. Proton Coupled Electronic Rearrangement within the H-Cluster as an Essential Step in the Catalytic Cycle of [FeFe] Hydrogenases. *J. Am. Chem. Soc.* **2017**, *139* (4), 1440–1443. doi: 10.1021/jacs.6b12636
(19) Mulder, D. W.; Boyd, E. S.; Sarma, R.; Lange, R. K.; Endrizzi, J. A.; Broderick, J. B.; Peters, J. W. Stepwise [FeFe]-Hydrogenase H-Cluster Assembly Revealed in the Structure of HydA(DeltaEFG). *Nature* **2010**, *465* (7295), 248–251. doi: 10.1038/nature08993
(20) Nicolet, Y.; Piras, C.; Legrand, P.; Hatchikian, C. E.; Fontecilla-Camps, J. C. Desulfovibrio Desulfuricans Iron Hydrogenase: The Structure Shows Unusual Coordination to an Active Site Fe Binuclear Center. *Structure* **1999**, *7* (1), 13–23. doi: 10.1016/s0969-2126(99)80005-7
(21) Rodríguez-Maciá, P.; Galle, L. M.; Bjornsson, R.; Lorent, C.; Zebger, I.; Yoda, Y.; Cramer, S. P.; DeBeer, S.; Span, I.; Birrell, J. A. Caught in the Hinact : Crystal Structure and Spectroscopy Reveal a Sulfur Bound to the Active Site of an O2 -Stable State of [FeFe] Hydrogenase. *Angew. Chem. Int. Ed Engl.* **2020**, *59* (38), 16786–16794. doi: 10.1002/anie.202005208
(22) Rodríguez-Maciá, P.; Reijerse, E. J.; van Gastel, M.; DeBeer, S.; Lubitz, W.; Rüdiger, O.; Birrell, J. A. Sulfide Protects [FeFe] Hydrogenases From O2. *J. Am. Chem. Soc.* **2018**, *140* (30), 9346–9350. doi: 10.1021/jacs.8b04339
(23) Kubas, A.; Orain, C.; De Sancho, D.; Saujet, L.; Sensi, M.; Gauquelin, C.; Meynial-Salles, I.; Soucaille, P.; Bottin, H.; Baffert, C.; Fourmond, V.; Best, R. B.; Blumberger, J.; Léger, C. Mechanism of O2 Diffusion and Reduction in FeFe Hydrogenases. *Nat. Chem.* **2017**, *9* (1), 88–95. doi: 10.1038/nchem.2592
(24) Hatchikian, E. C.; Forget, N.; Fernandez, V. M.; Williams, R.; Cammack, R. Further Characterization of the [Fe]-Hydrogenase from Desulfovibrio Desulfuricans ATCC 7757. *Eur. J. Biochem.* **1992**, *209* (1), 357–365. doi: 10.1111/j.1432-1033.1992.tb17297.x
(25) Roseboom, W.; De Lacey, A. L.; Fernandez, V. M.; Hatchikian, E. C.; Albracht, S. P. J. The Active Site of the [FeFe]-Hydrogenase from Desulfovibrio Desulfuricans. II. Redox Properties, Light Sensitivity and CO-Ligand Exchange as Observed by Infrared Spectroscopy. *J. Biol. Inorg. Chem.* **2006**, *11* (1), 102–118. doi: 10.1007/s00775-005-0040-2
(26) Patil, D. S.; Moura, J. J.; He, S. H.; Teixeira, M.; Prickril, B. C.; DerVartanian, D. V.; Peck, H. D., Jr; LeGall, J.; Huynh, B. H. EPR-Detectable Redox Centers of the Periplasmic Hydrogenase from Desulfovibrio Vulgaris. *J. Biol. Chem.* **1988**, *263*

(35), 18732–18738. doi: 10.1016/S0021-9258(18)37344-7
(27) Pierik, A. J.; Hagen, W. R.; Redeker, J. S.; Wolbert, R. B.; Boersma, M.; Verhagen, M. F.; Grande, H. J.; Veeger, C.; Mutsaers, P. H.; Sands, R. H. Redox Properties of the Iron-Sulfur Clusters in Activated Fe-Hydrogenase from Desulfovibrio Vulgaris (Hildenborough). *Eur. J. Biochem.* **1992**, *209* (1), 63–72. doi: 10.1111/j.1432-1033.1992.tb17261.x
(28) Pereira, A. S.; Tavares, P.; Moura, I.; Moura, J. J.; Huynh, B. H. Mössbauer Characterization of the Iron-Sulfur Clusters in Desulfovibrio Vulgaris Hydrogenase. *J. Am. Chem. Soc.* **2001**, *123* (12), 2771–2782. doi: 10.1021/ja003176+
(29) Albracht, S. P. J.; Roseboom, W.; Hatchikian, E. C. The Active Site of the [FeFe]-Hydrogenase from Desulfovibrio Desulfuricans. I. Light Sensitivity and Magnetic Hyperfine Interactions as Observed by Electron Paramagnetic Resonance. *J. Biol. Inorg. Chem.* **2006**, *11* (1), 88–101. doi: 10.1007/s00775-005-0039-8
(30) May, P. M.; Batka, D.; Hefter, G.; Königsberger, E.; Rowland, D. Goodbye to S2- in Aqueous Solution. *Chem. Commun.* **2018**, *54* (16), 1980–1983. doi: 10.1039/c8cc00187a
(31) Winkler, M.; Duan, J.; Rutz, A.; Felbek, C.; Scholtysek, L.; Lampret, O.; Jaenecke, J.; Apfel, U.-P.; Gilardi, G.; Valetti, F.; Fourmond, V.; Hofmann, E.; Léger, C.; Happe, T. A Safety Cap Protects Hydrogenase from Oxygen Attack. *Nat. Commun.* **2021**, *12* (1), 756. doi: 10.1038/s41467-020-20861-2
(32) Corrigan, P. S.; Tirsch, J. L.; Silakov, A. Investigation of the Unusual Ability of the [FeFe] Hydrogenase from Clostridium Beijerinckii to Access an O2-Protected State. *J. Am. Chem. Soc.* **2020**, *142* (28), 12409–12419. doi: 10.1021/jacs.0c04964
(33) Haynes, W. M. *CRC Handbook of Chemistry and Physics*; CRC Press, 2016, page D-119.
(34) Del Barrio, M.; Sensi, M.; Orain, C.; Baffert, C.; Dementin, S.; Fourmond, V.; Léger, C. Electrochemical Investigations of Hydrogenases and Other Enzymes That Produce and Use Solar Fuels. *Acc. Chem. Res.* **2018**, *51* (3), 769–777. doi: 10.1021/acs.accounts.7b00622
(35) Sensi, M.; del Barrio, M.; Baffert, C.; Fourmond, V.; Léger, C. New Perspectives in Hydrogenase Direct Electrochemistry. *Current Opinion in Electrochemistry* **2017**, *5* (1), 135–145. doi: 10.1016/j.coelec.2017.08.005
(36) Léger, C.; Bertrand, P. Direct Electrochemistry of Redox Enzymes as a Tool for Mechanistic Studies. *Chem. Rev.* **2008**, *108* (7), 2379–2438. doi: 10.1021/cr0680742
(37) Del Barrio, M.; Sensi, M.; Fradale, L.; Bruschi, M.; Greco, C.; de Gioia, L.; Bertini, L.; Fourmond, V.; Léger, C. Interaction of the H-Cluster of FeFe Hydrogenase with Halides. *J. Am. Chem. Soc.* **2018**, *140* (16), 5485–5492. doi: 10.1021/jacs.8b01414
(38) Perrin, D. D. *Ionisation Constants of Inorganic Acids and Bases in Aqueous Solution*; Solubility Data Series; Pergamon, 2013.
(39) Léger, C.; Dementin, S.; Bertrand, P.; Rousset, M.; Guigliarelli, B. Inhibition and Aerobic Inactivation Kinetics of Desulfovibrio Fructosovorans NiFe Hydrogenase Studied by Protein Film Voltammetry. *J. Am. Chem. Soc.* **2004**, *126* (38), 12162–12172. doi: 10.1021/ja046548d
(40) Benvenuti, M.; Meneghello, M.; Guendon, C.; Jacq-Bailly, A.; Jeoung, J.-H.; Dobbek, H.; Léger, C.; Fourmond, V.; Dementin, S. The Two CO-Dehydrogenases of Thermococcus Sp. AM4. *Biochim. Biophys. Acta Bioenerg.* **2020**, *1861* (7), 148188. doi: 10.1016/j.bbabio.2020.148188
(41) Barrio, M.; Fourmond, V. Redox (in)activations of Metalloenzymes: A Protein Film Voltammetry Approach. *ChemElectroChem* **2019**, *6* (19), 4949–4962. doi: 10.1002/celc.201901028
(42) Baffert, C.; Bertini, L.; Lautier, T.; Greco, C.; Sybirna, K.; Ezanno, P.; Etienne, E.; Soucaille, P.; Bertrand, P.; Bottin, H.; Meynial-Salles, I.; De Gioia, L.; Léger, C. CO Disrupts the Reduced H-Cluster of FeFe Hydrogenase. A Combined DFT and Protein Film Voltammetry Study. *J. Am. Chem. Soc.* **2011**, *133* (7), 2096–2099. doi: 10.1021/ja110627b
(43) Fourmond, V.; Baffert, C.; Sybirna, K.; Dementin, S.; Abou-Hamdan, A.; Meynial-Salles, I.; Soucaille, P.; Bottin, H.; Léger, C. The Mechanism of Inhibition by H2 of H2-Evolution by Hydrogenases. *Chem. Commun.* **2013**, *49* (61), 6840–6842. doi: 10.1039/c3cc43297a
(44) Sensi, M.; Baffert, C.; Greco, C.; Caserta, G.; Gauquelin, C.; Saujet, L.; Fontecave, M.; Roy, S.; Artero, V.; Soucaille, P.; Meynial-Salles, I.; Bottin, H.; de Gioia, L.; Fourmond, V.; Léger, C.; Bertini, L. Reactivity of the Excited States of the H-Cluster of FeFe Hydrogenases. *J. Am. Chem. Soc.* **2016**, *138* (41), 13612–13618. doi: 10.1021/jacs.6b06603
(45) Jones, A. K.; Lamle, S. E.; Pershad, H. R.; Vincent, K. A.; Albracht, S. P. J.; Armstrong, F. A. Enzyme Electrokinetics: Electrochemical Studies of the Anaerobic Interconversions between Active and Inactive States of Allochromatium Vinosum [NiFe]-Hydrogenase. *J. Am. Chem. Soc.* **2003**, *125* (28), 8505–8514. doi: 10.1021/ja035296y
(46) Fourmond, V.; Infossi, P.; Giudici-Orticoni, M.-T.; Bertrand, P.; Léger, C. "Two-Step" Chronoamperometric Method for Studying the Anaerobic Inactivation of an Oxygen Tolerant NiFe Hydrogenase. *J. Am. Chem. Soc.* **2010**, *132* (13), 4848–4857. doi: 10.1021/ja910685j
(47) Abou Hamdan, A.; Liebgott, P.-P.; Fourmond, V.; Gutiérrez-Sanz, O.; De Lacey, A. L.; Infossi, P.; Rousset, M.; Dementin, S.; Léger, C. Relation between Anaerobic Inactivation and Oxygen Tolerance in a Large Series of NiFe Hydrogenase Mutants. *Proc. Natl. Acad. Sci. U. S. A.* **2012**, *109* (49), 19916–19921. doi: 10.1073/pnas.1212258109
(48) Ceccaldi, P.; Marques, M. C.; Fourmond, V.; Pereira, I. C.; Léger, C. Oxidative Inactivation of NiFeSe Hydrogenase. *Chem. Commun.* **2015**, *51* (75), 14223–14226. doi: 10.1039/c5cc05930e
(49) Orain, C.; Saujet, L.; Gauquelin, C.; Soucaille, P.; Meynial-Salles, I.; Baffert, C.; Fourmond, V.; Bottin, H.; Léger, C. Electrochemical Measurements of the Kinetics of Inhibition of Two FeFe Hydrogenases by O2 Demonstrate That the Reaction Is Partly Reversible. *J. Am. Chem. Soc.* **2015**, *137* (39), 12580–12587. doi: 10.1021/jacs.5b06934
(50) Pandelia, M.-E.; Fourmond, V.; Tron-Infossi, P.; Lojou, E.; Bertrand, P.; Léger, C.; Giudici-Orticoni, M.-T.; Lubitz, W.

Membrane-Bound Hydrogenase I from the Hyperthermophilic Bacterium Aquifex Aeolicus: Enzyme Activation, Redox Intermediates and Oxygen Tolerance. *J. Am. Chem. Soc.* **2010**, *132* (20), 6991–7004. doi: 10.1021/ja910838d
(51) Thauer, R. K.; Käufer, B.; Zähringer, M.; Jungermann, K. The Reaction of the Iron-Sulfur Protein Hydrogenase with Carbon Monoxide. *Eur. J. Biochem.* **1974**, *42* (2), 447–452. doi: 10.1111/j.1432-1033.1974.tb03358.x
(52) Fersht, A.; University Alan Fersht. *Structure and Mechanism in Protein Science: A Guide to Enzyme Catalysis and Protein Folding*; W. H. Freeman, 1999.
(53) Almeida, M. G.; Silveira, C. M.; Guigliarelli, B.; Bertrand, P.; Moura, J. J. G.; Moura, I.; Léger, C. A Needle in a Haystack: The Active Site of the Membrane-Bound Complex Cytochrome c Nitrite Reductase. *FEBS Lett.* **2007**, *581* (2), 284–288. doi: 10.1016/j.febslet.2006.12.023
(54) Caserta, G.; Adamska-Venkatesh, A.; Pecqueur, L.; Atta, M.; Artero, V.; Roy, S.; Reijerse, E.; Lubitz, W.; Fontecave, M. Chemical Assembly of Multiple Metal Cofactors: The Heterologously Expressed Multidomain [FeFe]-Hydrogenase from Megasphaera Elsdenii. *Biochim. Biophys. Acta* **2016**, *1857* (11). doi: 10.1016/j.bbabio.2016.07.002
(55) Esselborn, J.; Muraki, N.; Klein, K.; Engelbrecht, V.; Metzler-Nolte, N.; Apfel, U. P.; Hofmann, E.; Kurisu, G.; Happe, T. A Structural View of Synthetic Cofactor Integration into [FeFe]-Hydrogenases. *Chem. Sci.* **2016**, *7* (2). doi: 10.1039/c5sc03397g
(56) Ikeda, S.; Satake, H.; Hisano, T.; Terazawa, T. Potentiometric Argentimetric Method for the Successive Titration of Sulphide and Dissolved Sulphur in Polysulphide Solutions. *Talanta* **1972**, *19* (12), 1650–1654. doi: 10.1016/0039-9140(72)80240-6
(57) Greiner, R.; Pálinkás, Z.; Bäsell, K.; Becher, D.; Antelmann, H.; Nagy, P.; Dick, T. P. Polysulfides Link H2S to Protein Thiol Oxidation. *Antioxid. Redox Signal.* **2013**, *19* (15), 1749–1765. doi: 10.1089/ars.2012.5041
(58) Best, R. B.; Mittal, J. Protein Simulations with an Optimized Water Model: Cooperative Helix Formation and Temperature-Induced Unfolded State Collapse. *J. Phys. Chem. B* **2010**, *114* (46), 14916–14923. doi: 10.1021/jp108618d
(59) Abascal, J. L. F.; Vega, C. A General Purpose Model for the Condensed Phases of Water: TIP4P/2005. *J. Chem. Phys.* **2005**, *123* (23), 234505. doi: 10.1063/1.2121687
(60) Chang, C. H.; Kim, K. Density Functional Theory Calculation of Bonding and Charge Parameters for Molecular Dynamics Studies on [FeFe] Hydrogenases. *J. Chem. Theory Comput.* **2009**, *5* (4), 1137–1145. doi: 10.1021/ct800342w
(61) Galvelis, R.; Doerr, S.; Damas, J. M.; Harvey, M. J.; De Fabritiis, G. A Scalable Molecular Force Field Parameterization Method Based on Density Functional Theory and Quantum-Level Machine Learning. *J. Chem. Inf. Model.* **2019**, *59* (8), 3485–3493. doi: 10.1021/acs.jcim.9b00439
(62) Cohen, J.; Kim, K.; King, P.; Seibert, M.; Schulten, K. Finding Gas Diffusion Pathways in Proteins: Application to O2 and H2 Transport in CpI [FeFe]-Hydrogenase and the Role of Packing Defects. *Structure* **2005**, *13* (9), 1321–1329. doi: 10.1016/j.str.2005.05.013
(63) Lambertz, C.; Chernev, P.; Klingan, K.; Leidel, N.; Sigfridsson, K. G. V.; Happe, T.; Haumann, M. Electronic and Molecular Structures of the Active-Site H-Cluster in [FeFe]-Hydrogenase Determined by Site-Selective X-Ray Spectroscopy and Quantum Chemical Calculations. *Chem. Sci.* **2014**, *5* (3), 1187–1203. doi: 10.1039/C3SC52703D
(64) Birrell, J. A.; Pelmenschikov, V.; Mishra, N.; Wang, H.; Yoda, Y.; Tamasaku, K.; Rauchfuss, T. B.; Cramer, S. P.; Lubitz, W.; DeBeer, S. Spectroscopic and Computational Evidence That [FeFe] Hydrogenases Operate Exclusively with CO-Bridged Intermediates. *J. Am. Chem. Soc.* **2020**, *142* (1), 222–232. doi: 10.1021/jacs.9b09745
(65) Almazahreh, L. R.; Arrigoni, F.; Abul-Futouh, H.; El-khateeb, M.; Görls, H.; Elleouet, C.; Schollhammer, P.; Bertini, L.; De Gioia, L.; Rudolph, M.; Zampella, G.; Weigand, W. Proton Shuttle Mediated by (SCH2)2P═O Moiety in [FeFe]-Hydrogenase Mimics: Electrochemical and DFT Studies. *ACS Catalysis*. 2021, pp 7080–7098. doi: 10.1021/acscatal.0c05563
(66) Breglia, R.; Arrigoni, F.; Sensi, M.; Greco, C.; Fantucci, P.; De Gioia, L.; Bruschi, M. First-Principles Calculations on Ni,Fe-Containing Carbon Monoxide Dehydrogenases Reveal Key Stereoelectronic Features for Binding and Release of CO To/from the C-Cluster. *Inorg. Chem.* **2021**, *60* (1), 387–402. doi: 10.1021/acs.inorgchem.0c03034
(67) Raugei, S.; Seefeldt, L. C.; Hoffman, B. M. Critical Computational Analysis Illuminates the Reductive-Elimination Mechanism That Activates Nitrogenase for N Reduction. *Proc. Natl. Acad. Sci. U. S. A.* **2018**, *115* (45), E10521–E10530. doi: 10.1073/pnas.1810211115
(68) Bruschi, M.; Greco, C.; Bertini, L.; Fantucci, P.; Ryde, U.; De Gioia, L. Functionally Relevant Interplay between the Fe(4)S(4) Cluster and CN(-) Ligands in the Active Site of [FeFe]-Hydrogenases. *J. Am. Chem. Soc.* **2010**, *132* (14), 4992–4993. doi: 10.1021/ja1008773
(69) Cao, L.; Ryde, U. Extremely Large Differences in DFT Energies for Nitrogenase Models. *Phys. Chem. Chem. Phys.* **2019**, *21* (5), 2480–2488. doi: 10.1039/c8cp06930a
(70) Stripp, S. T.; Mebs, S.; Haumann, M. Temperature Dependence of Structural Dynamics at the Catalytic Cofactor of [FeFe]-Hydrogenase. *Inorg. Chem.* **2020**, *59* (22), 16474–16488. doi: 10.1021/acs.inorgchem.0c02316
(71) Senger, M.; Laun, K.; Wittkamp, F.; Duan, J.; Haumann, M.; Happe, T.; Winkler, M.; Apfel, U.-P.; Stripp, S. T. Proton-Coupled Reduction of the Catalytic [4Fe-4S] Cluster in [FeFe]-Hydrogenases. *Angewandte Chemie International Edition*. 2017, pp 16503–16506. doi: 10.1002/anie.201709910
(72) Rodríguez-Maciá, P.; Pawlak, K.; Rüdiger, O.; Reijerse, E. J.; Lubitz, W.; Birrell, J. A. Intercluster Redox Coupling Influences Protonation at the H-Cluster in [FeFe] Hydrogenases. *Journal of the American Chemical Society*. 2017, pp 15122–15134. doi: 10.1021/jacs.7b08193
(73) Artz, J. H.; Zadvornyy, O. A.; Mulder, D. W.; Keable, S. M.; Cohen, A. E.; Ratzloff, M. W.; Williams, S. G.; Ginovska, B.; Kumar, N.; Song, J.; McPhillips, S. E.; Davidson, C. M.; Lyubimov, A. Y.; Pence, N.; Schut, G. J.; Jones, A. K.; Soltis, S. M.;

Adams, M. W. W.; Raugei, S.; King, P. W.; Peters, J. W. Tuning Catalytic Bias of Hydrogen Gas Producing Hydrogenases. *J. Am. Chem. Soc.* **2020**, *142* (3), 1227–1235. doi: 10.1021/jacs.9b08756

(74) Duan, J.; Mebs, S.; Laun, K.; Wittkamp, F.; Heberle, J.; Happe, T.; Hofmann, E.; Apfel, U.-P.; Winkler, M.; Senger, M.; Haumann, M.; Stripp, S. T. Geometry of the Catalytic Active Site in [FeFe]-Hydrogenase Is Determined by Hydrogen Bonding and Proton Transfer. *ACS Catal.* **2019**, *9* (10), 9140–9149. doi: 10.1021/acscatal.9b02203

(75) Stripp, S. T. In Situ Infrared Spectroscopy for the Analysis of Gas-Processing Metalloenzymes. *ACS Catal.* **2021**, 7845–7862. doi: 10.1021/acscatal.1c00218

(76) Blackmond, D. G. "If Pigs Could Fly" Chemistry: A Tutorial on the Principle of Microscopic Reversibility. *Angew. Chem. Int. Ed Engl.* **2009**, *48* (15), 2648–2654. doi: 10.1002/anie.200804566

(77) Caserta, G.; Papini, C.; Adamska-Venkatesh, A.; Pecqueur, L.; Sommer, C.; Reijerse, E.; Lubitz, W.; Gauquelin, C.; Meynial-Salles, I.; Pramanik, D.; Artero, V.; Atta, M.; Del Barrio, M.; Faivre, B.; Fourmond, V.; Léger, C.; Fontecave, M. Engineering an [FeFe]-Hydrogenase: Do Accessory Clusters Influence O2 Resistance and Catalytic Bias? *J. Am. Chem. Soc.* **2018**, *140* (16), 5516–5526. doi: 10.1021/jacs.8b01689

(78) Oughli, A. A.; Hardt, S.; Rüdiger, O.; Birrell, J. A.; Plumeré, N. Reactivation of Sulfide-Protected [FeFe] Hydrogenase in a Redox-Active Hydrogel. *Chem. Commun.* **2020**, *56* (69), 9958–9961. doi: 10.1039/d0cc03155k